iScience

CellPress
OPEN ACCESS

Article

Drosophila p53 tumor suppressor directly activates conserved asymmetric stem cell division regulators

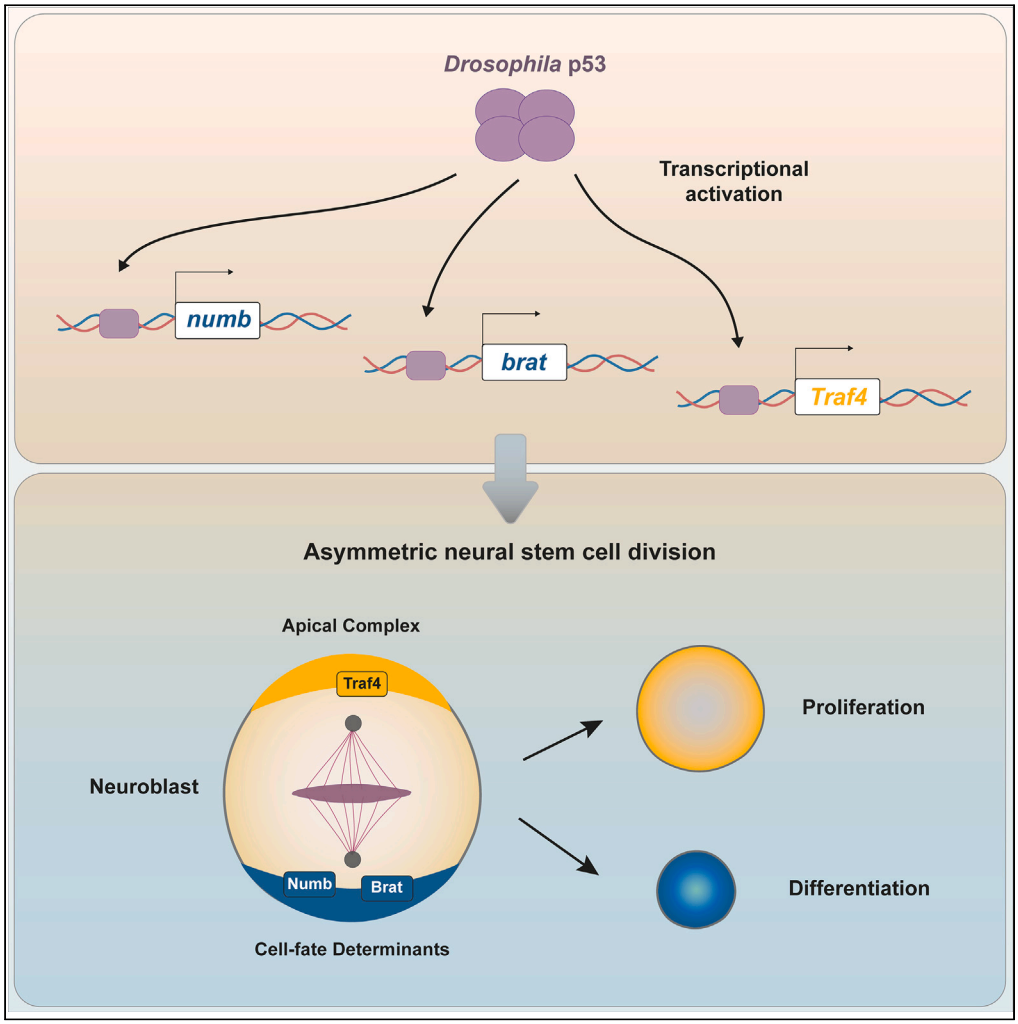

Sandra Manzanero-Ortiz, Maribel Franco, Mahima Laxmeesha, Ana Carmena

acarmena@umh.es

Highlights

Drosophila p53 regulates asymmetric stem cell division (ASCD)

Drosophila p53 directly activates Numb, Brat, and Traf4 ASCD regulators

Human and mice genes related to Brat and Traf4 are predicted conserved p53 targets

p53 loss might cooperate with other ASCD regulator mutations to induce tumoral growth

Manzanero-Ortiz et al., iScience *27*, 111118
November 15, 2024
https://doi.org/10.1016/j.isci.2024.111118

iScience

CellPress
OPEN ACCESS

Article

Drosophila p53 tumor suppressor directly activates conserved asymmetric stem cell division regulators

Sandra Manzanero-Ortiz,[1,2] Maribel Franco,[1,2] Mahima Laxmeesha,[1] and Ana Carmena[1,3,*]

SUMMARY

_p53_ is the most mutated tumor suppressor gene in human cancers. Besides p53 classical functions inducing cell-cycle arrest and apoptosis in stressed cells, additional p53 non-canonical roles in unstressed cells have emerged over the past years, including the mode of stem cell division regulation. However, the mechanisms by which p53 impacts on this process remain elusive. Here, we show that _Drosophila_ p53 controls asymmetric stem cell division (ASCD), a key process in development, cancer and adult tissue homeostasis, by transcriptionally activating Numb, Brat, and Traf4 ASCD regulators. _p53_ knockout caused failures in their localization in dividing neural stem cells, as well as a significant decrease in their expression levels. Moreover, p53 directly bound _numb_, _brat_, and _Traf4_ regulatory regions. Remarkably, human and mice genes related to _Drosophila brat_ (_TRIM32_) and _Traf4_ (_TRAF4_) were recently identified in a meta-analysis of transcriptomic and ChIP-seq datasets as predicted conserved p53 targets.

INTRODUCTION

Asymmetric stem cell division (ASCD) is an evolutionary conserved process to generate cell diversity during development and to regulate tissue homeostasis in the adult. Likewise, over the past years, it has been revealed the significance of ASCD in the context of stem and cancer cell biology.[1–9] The neural stem cells of the *Drosophila* central nervous system (CNS), called neuroblasts (NBs), constitute one of the main paradigms in which to study ASCD, including the Type I NBs (NBIs) of the *Drosophila* embryo.[10,11] These NBIs divide asymmetrically to generate another NB that keeps on self-renewing and a ganglion mother cell (GMC) that is committed to initiate a differentiation program. This GMC will divide only once more, asymmetrically, to give rise to two distinct neuron or glial cells (Figure 1A). The generation of two different daughter cells through an ASCD requires the participation of an intricate regulatory machinery. For example, the "apical complex," which includes small GTPases, an atypical protein kinase C (aPKC) and partitioning-defective (PAR) proteins,[12–19] is located at the apical pole of dividing NBs and promotes the basal displacement in metaphase NBs of the so-called cell-fate determinants (Figure 1A). These cell-fate determinants, such as the Notch inhibitor Numb and the translational regulator Brain Tumor (Brat)/TRIM3, TRIM2, and TRIM32 in humans, will exclusively segregate to the basal daughter cell, the GMC, committing this cell to leave the self-renewal program.[10,20–27] Hence, the ASCD regulatory network ensures a precise balance between cell proliferation and differentiation. In fact, failures in the process of ASCD can lead to tumor-like overgrowth.[28] Likewise, genes originally identified as tumor suppressors, such as *lethal (2) giant larvae* (*l(2)gl*)/LLGL1 in humans, *brat*, and *discs large1* (*dlg1*)/*DLG1*, were shown a posteriori to be key ASCD regulators.[20–23,29–35] Thus, an intriguing possibility is that other well-known tumor suppressor genes also participate in modulating ASCD in normal conditions.

Human *TP53* (*Trp53* in mice), which encodes the tumor suppressor protein p53 known as the "guardian of the genome," is the most mutated gene in human cancers.[36–40] Multiple cellular stress factors, including DNA damage, hypoxia, nutrient deprivation, and oncogene deregulation, lead to the stabilization and activation of p53, which is targeted for degradation by the E3 ubiquitin ligase MDM2 and, consequently, present at low levels in normal conditions.[41,42] p53 largely responds promoting cell-cycle arrest and apoptosis through transcriptionally activating a network of target genes.[43–45] However, since its discovery in 1979,[46–50] p53 has been shown to display additional functions in non-canonical programs such as autophagy, inflammation, and metabolism. Likewise, novel roles of p53 in unstressed cells, during embryonic development and differentiation and in stem cell populations, have been emerging over the past decades.[3,37,43,51–61] Despite the low sequence conservation and the evolutionary distance, the *Drosophila* gene *p53* is the structural and functional homolog of the human *TP53*.[62,63] For example, *Drosophila* p53 is also a key inductor of apoptosis[64,65] but, unlike human p53, is not involved in DNA-damage-induced cell-cycle arrest.[64,65] However, *Drosophila* p53 does regulate cell-cycle progression in specific stress conditions, such as mitochondria dysfunction.[66] Also, even though a clear MDM2 homolog has not been found in the *Drosophila* genome, other ubiquitin ligases or negative regulators of *Drosophila* p53, functionally equivalents, have been described.[64,67,68] *Drosophila* p53 has also contributed to the characterization of p53 novel non-canonical functions, including cell

[1]Instituto de Neurociencias, Consejo Superior de Investigaciones Científicas/Universidad Miguel Hernández de Elche, Sant Joan d'Alacant, 03550 Alicante, Spain
[2]These authors contributed equally
[3]Lead contact
*Correspondence: acarmena@umh.es
https://doi.org/10.1016/j.isci.2024.111118

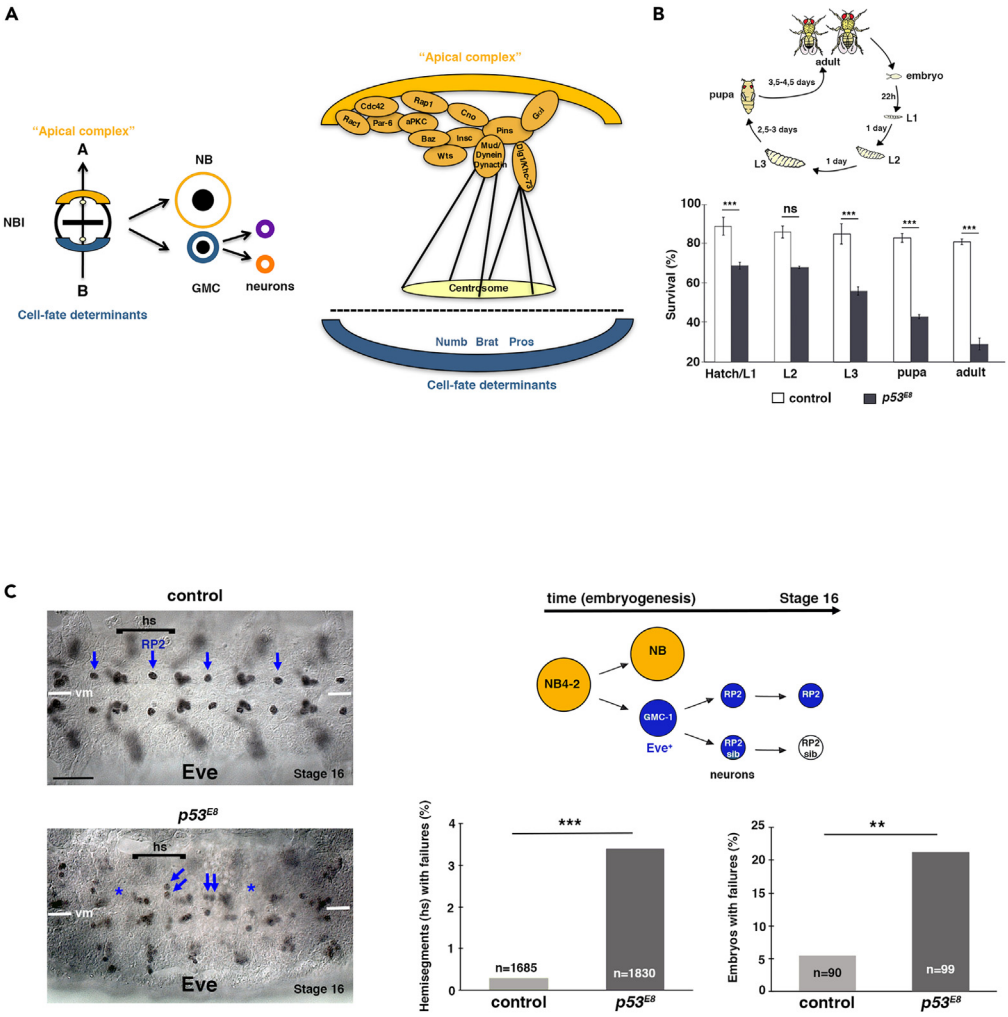

Figure 1. p53 is required for proper neuronal lineage formation

(A) NB asymmetric division is regulated by an "apical complex" and cell-fate determinants that localize asymmetrically at the apical and basal poles, respectively, of metaphase NBs. NBI asymmetric division renders another NB and a GMC, which receives the determinants and stops self-renewing. The GMC through a terminal asymmetric division generates two different neurons or glial cells: (A) apical, (B) basal.

(B) *p53* homozygous null mutant viability strongly decays throughout *Drosophila* life cycle (upper diagram). A significant number of *p53* homozygous embryos do not hatch compared to control embryos; no significant (ns) changes in the survival of *p53* mutants are observed from L1 to L2 larvae; very significant decay in the survival of *p53* mutants is observed again since L3 to the adult eclosion compared to the control. Data are represented as mean ± SD (standard deviation); $n = 2$ independent experiments (***$p < 0.001$).

(C) Ventral views of late stage *Drosophila* embryos, control, and $p53^{E8}$ homozygous null mutants, showing different hemisegments (hs) at each side of the ventral midline (vm). In control embryos, the transcription factor Eve is expressed in a subset of neurons, including one RP2 neuron per hs (blue arrows); in $p53^{E8}$ mutants, a significant number (***$p < 0.001$; **$p < 0.01$ in the bar graphs) of RP2 duplications (blue arrows in the picture) or losses (blue asterisks) are detected. A diagram of the GMC-1 neuronal lineage is represented. n = number of total hemisegments (hs) or embryos. Scale bar: 20 μm.

competition, coordination of tissue growth, and metabolic homeostasis.[69–71] Thus, given the shared functional homologies, the simplicity of *Drosophila* p53 family (only one member versus three: p53, p63, and p73, in humans), along with *Drosophila* suitability for genetic manipulation, *Drosophila* p53 is still an appealing model system to get deep insight into human TP53 functionality.[58,63,72] Here, we show that *Drosophila* p53 controls ASCD by transcriptionally activating Numb, Brat, and Traf4, key ASCD regulators whose human and mice homologues have been recently identified in a meta-analysis of transcriptomic and ChIP-seq datasets as predicted conserved p53 targets.[73]

RESULTS

p53 homozygous null mutant viability strongly decays throughout *Drosophila* life cycle

It has been reported that *Drosophila* p53 is not essential for normal development; even though flies lacking p53 show a reduced ability to respond to stress signals, they survive displaying only mild defects in longevity and fertility.[65,74] However, we observed that it was very

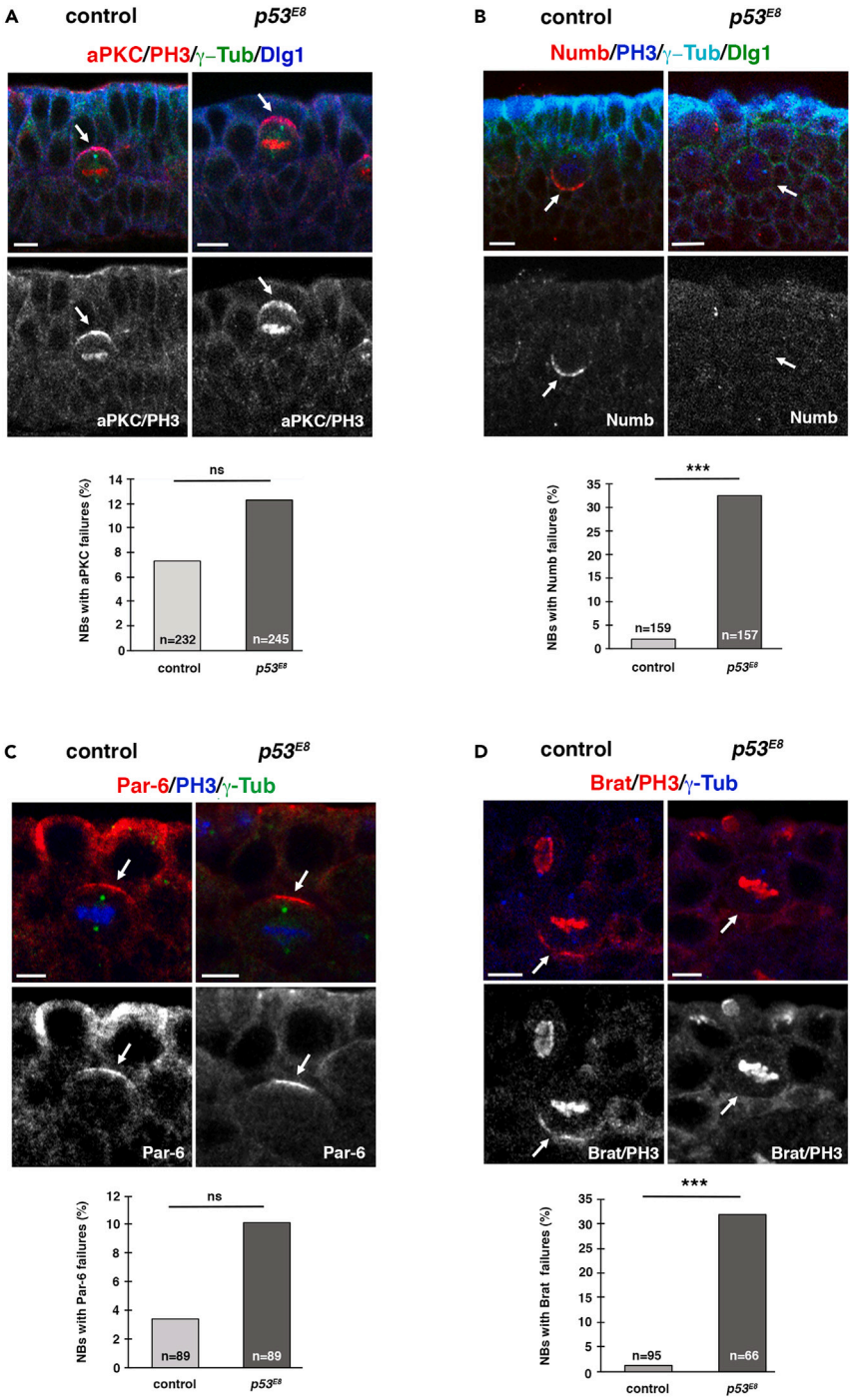

Figure 2. *Drosophila* p53 impacts the localization of the ASCD regulators Numb and Brat in dividing NBs

(A) Confocal immunofluorescences showing an embryonic metaphase NB in control or $p53^{E8}$ homozygous mutants stained with the apical protein aPKC (in red; arrow); mitotic cells are visualized with PH3 (red), centrosomes are labeled with γ-Tub (green), and membranes are marked by Dlg1 (blue). No significant (ns) defects in the apical localization of aPKC are detected in $p53^{E8}$ mutants.

(B) Confocal immunofluorescences showing an embryonic metaphase NB in control or $p53^{E8}$ homozygous mutants stained with the cell fate determinant Numb (red; arrow); mitotic cells are visualized with PH3 (blue), centrosomes are labeled with γ-Tub (light blue), and membranes are marked by Dlg1 (green). Numb localization is significantly altered (***$p < 0.001$ in the bar graph) in $p53^{E8}$ homozygotes.

Figure 2. *Continued*

(C) Confocal immunofluorescences showing an embryonic metaphase NB in control or $p53^{E8}$ homozygous mutants stained with the apical protein Par-6 (in red; arrow); mitotic cells are visualized with PH3 (blue), and centrosomes are labeled with γ-Tub (green). No significant (ns) defects in the apical localization of Par-6 are detected in $p53^{E8}$ homozygous mutants.

(D) Confocal immunofluorescences showing an embryonic metaphase NB in control or $p53^{E8}$ homozygous mutants stained with the cell fate determinant Brat (red; arrow); mitotic cells are visualized with PH3 (red), and centrosomes are labeled with γ-Tub (blue). Brat localization is significantly altered (***$p < 0.001$ in the bar graph) in $p53^{E8}$ homozygote mutants. n = number of metaphase NBs analyzed; scale bar: 5 μm. See also Figures S1 and S3.

problematic to maintain a stock of *p53* homozygous null mutant flies for a long time. Thus, we performed a viability assay throughout the *Drosophila* life cycle, finding an increased mortality of *p53* mutants with respect to the control at different stages of the cycle, from embryo until adult hatching (Figure 1B). This result suggested that the loss of *p53* entails a sensitized genetic background, a disadvantage for fitness and survival throughout *Drosophila* life cycle. Thus, we started looking at potential phenotypes of *p53* null mutants in the *Drosophila* embryo.

p53 is required for proper neuronal lineage formation

The embryonic *Drosophila* GMC-1 neuronal lineage has been extensively studied.[75–77] This GMC expresses the transcription factor Even-Skipped (Eve) and divides asymmetrically to give rise to two different neurons called RP2 and RP2 sibling. Both neurons express Eve initially but, at later stages of embryogenesis, only RP2 keeps expressing Eve. Thus, under normal conditions, at these later stages only one Eve^{+} RP2 neuron is present per hemisegment (Figure 1C). However, defects in the number of RP2 neurons (i.e., either losses or duplications) are detected in mutant embryos for ASCD regulators.[78–82] We observed that $p53^{E8}$ homozygous null mutant embryos ($n = 99$) displayed defects in the number of RP2s in a significant number of hemisegments ($n = 1830$) compared to control embryos ($n = 90$; $n = 1685$ hemisegments) (Figure 1C). This result suggested that p53 might be regulating the ASCD within the GMC-1 neuronal lineage in normal conditions.

p53 impacts on the localization of the ASCD regulator Numb in dividing NBs

To more directly support a potential function of p53 in ASCD, we decided to look at the localization of central ASCD regulators, such as the apical complex protein aPKC and the cell-fate determinant Numb (Figure 1A), in dividing NBs at earlier stages of embryogenesis. No significant defects were detected in the apical localization of aPKC in $p53^{E8}$ mutant metaphase NBs ($n = 245$ NBs; 24 embryos) compared to control NBs ($n = 232$; 27 embryos) (Figure 2A). However, the localization of Numb, present in a basal crescent in control metaphase NBs ($n = 159$ NBs; 28 embryos), was compromised in $p53^{E8}$ mutant embryos ($n = 157$ metaphase NBs; 24 embryos) (Figure 2B). Intriguingly, almost all the failures observed (96,1%; 49/51 of the metaphase NBs with defective Numb) were "absence" of Numb, suggesting that p53 might be directly or indirectly regulating the expression of Numb.

Drosophila homologues of conserved human/mice predicted p53 targets regulate ASCD

Next, we wondered whether, apart from Numb, other ASCD regulators might be regulated by p53. Instead of a random analysis, we decided to follow an *in silico* approach, taking advantage of published datasets about potential p53 target genes. It was particularly interesting a recent meta-analysis of transcriptomic and ChIP-seq datasets in which the author unveiled a subset of 86 direct p53 target genes commonly predicted in mice and humans.[73] Hence, we decided looking for those human/mice genes whose closest counterparts in *Drosophila* are ASCD regulators. We focused on three of these genes for further analyses: *TRIM32*, *PARD6G*, and *TRAF4*. TRIM32 is related to *Drosophila* Brat, an atypical TRIM-NHL protein (Brat lacks the RING domain normally present in these proteins) and, like Numb, a key cell-fate determinant during asymmetric NB division[20–23] (Figure 1A). PARD6G is homologue of *Drosophila* Par-6, which forms part of the apical complex in dividing NBs,[13] and the TRAF4 counterpart in *Drosophila*, Traf4, is another apical regulator required in the telophase rescue pathway during asymmetric NB division.[83] Thus, we started analyzing the localization of these *Drosophila* regulators in metaphase NBs. The localization of Par-6 was not affected in mitotic NBs ($n = 89$) of $p53^{E8}$ mutant embryos ($n = 14$) (Figure 2C). However, we detected a significant number of failures in the basal localization of Brat in metaphase NBs ($n = 66$) of $p53^{E8}$ mutant embryos ($n = 11$) compared with control embryos (Figure 2D). Most of the defects in Brat localization were "absence" (47.6% of the metaphase NBs with defects) or Brat mislocalization (42.9% of defective NBs). Intriguingly, both Brat and Numb localization defects (see above) in metaphase NBs were partially recovered at telophase, a phenomenon known as "telophase rescue"[31] (Figure S1). We could not analyze Traf4 localization as we were not able to generate appropriate antibodies to reproduce the published expression pattern of Traf4 in NBs.[83]

Drosophila p53 regulates the expression of the ASCD regulators Numb, Brat, and Traf4

To determine whether p53 was transcriptionally regulating Numb and Brat, we performed quantitative polymerase chain reaction (qPCR) analyses to determine their expression levels in $p53^{E8}$ homozygous mutant versus control larvae. We also included Traf4 in this set of experiments. We observed a significant reduction in all *numb*, *brat*, and *Traf4* expression levels in $p53^{E8}$ homozygous mutants (Figure 3A and Table 1). Hence, p53, directly or indirectly, regulates the expression of the ASCD regulators Numb, Brat, and Traf4.

Drosophila p53 directly binds to *numb*, *brat*, and *Traf4* regulatory regions

Next, we wanted to clarify whether p53 was activating the expression of *numb*, *brat*, and *Traf4* by directly binding to each of their regulatory regions. With that aim, we performed chromatin immunoprecipitation (ChIP) experiments. First, we analyzed the genomic regions

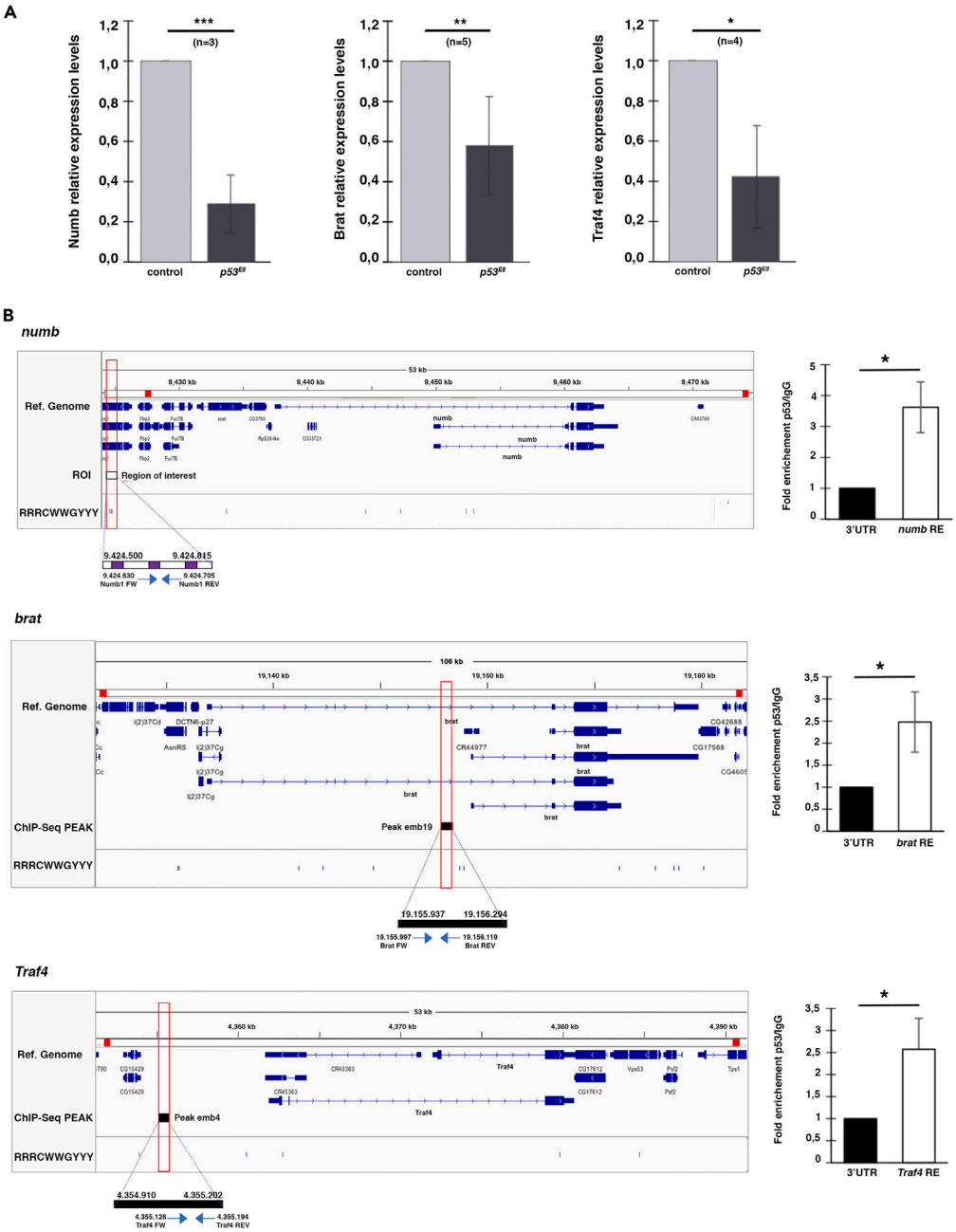

Figure 3. *Drosophila* p53 directly activates the ASCD regulators Numb, Brat, and Traf4

(A) RT-qPCRs reveal a significant decrease in the level of expression of the indicated genes in $p53^{E8}$ null homozygotes relative to the control. *$p < 0.05$, **$p < 0.01$, ***$p < 0.001$; data are represented as mean ± SD (standard deviation); n indicates the number of experiments (RT-qPCRs) performed for each gene.

(B) Visualization of ChIP-seq data using the Integrative Genomics Viewer (IGV) browser, showing the peaks or regions of interest (ROIs) for p53 binding at the genomes of *numb*, *brat*, and *Traf4* in about 10 kb (region delimited by red dots) from which the transcription starts (see also Figure S2). Selected peaks or ROIs are highlighted by red open rectangles, and magnification of them are shown indicating, in each case, the primers used to validate those regions. Bar graphs show the quantification of the ChIP-qPCR experiments measuring p53 occupancy at the *brat*, *Traf4*, and *numb* REs. Positive control (corresponding to a p53 RE in the promoter, see Figure S2A) and negative control regions (the p53 3′UTR without any p53 REs) were included. Values in the graphs represent the fold enrichment observed using the p53 Ab for the immunoprecipitation with respect to an unspecific immunoglobulin G (IgG). Data are represented as mean ± SD (standard deviation); $n = 3$ independent experiments. A t test was used (*$p < 0.05$). See also Figure S2.

Table 1. Primers used for the RT-qPCR experiments

Gene	Fw primer	Rev primer
numb	GCA GCA TTA ATC AGA ACA TC	ATG GAG CGT CTG ATA TGT GG
brat	GCA AGG TGA TGC GTG TGA TC	TGT CGC TGA TGA AGA TCT CC
Traf4	GCA CTC TGT TGT GGA AGA TC	AGT GTG AAG GTG ATG GAG TGC
Act88F	TCG ATC ATG AAG TGC GAC GT	CGG AGT ACT TCC TCT CGG GT
GADPH	TAA ATT CGA CTC GAC TCA CGG T	CTC CAC CAC ATA CTC GGC TC

(about 10 Kb) around the genes searching for p53 response elements (REs) or closely related sequences. These REs were originally defined as two decameric repeats of the sequence RRRCWWGYYY, where R = A or G; W = A or T; and Y= C or T, separated by 0–18 bp,[84] though other combinations, such as only one decameric repeat, have also been found in p53 target genes.[85–87] To strengthen the selection of these regions, we also look in the Gene Expression Omnibus (GEO) repository and the Encyclopedia of DNA Elements (ENCODE) Consortium Project for available *p53* ChIP-seq datasets in *Drosophila*. Likewise, we took advantage of available data about epigenetic markers for open active chromatin, as well as from the genomic regions bound by the p53 partner E2F2 (Figure S2B)[88,89] to design pairs of primers for our ChIP experiments (Table 2). We identified several bona-fide p53 REs in all three regulatory regions (both upstream or/and in intron regions of each gene) (Figure 3B). In the case of Brat and Traf4, we focused on Peak regions previously identified in other ChIP-seq datasets to design the primers. (Figures 3B and S2B). For Numb, we selected a region in which we detected three decameric repeats RRRCWWGYYY, each separated by 80 nucleotides; additionally, in the first two repeats RRRCWWGYYY, the central motif CWWG was CAAG, which is predominantly found in p53 target genes[85] (Figure 3B). A specific mouse anti-p53 and an unspecific mouse IgG (as a negative control) were used in parallel to immunoprecipitate the chromatin from wild-type larval tissue. As p53 is known to regulate its own expression,[90–92] p53 was also included in the experiments as a positive control (Figure S2A). All the values for the different target regions were normalized against a p53 3'UTR region that is not recognized by p53. A significant enrichment in the regulatory regions of all three genes, *numb*, *brat*, and *Traf4* were detected in the immunoprecipitates. (Figure 3B). Thus, *Drosophila* p53 directly binds to *numb*, *brat*, and *Traf4* regulatory regions.

p53 loss does not induce tumor-like overgrowth in larval brains

Compromising ASCD can lead to tumor-like overgrowth.[28] Given the role of p53 as an ASCD regulator that we had observed, we next wanted to analyze the consequences of eliminating *p53* in the growth of NB lineages. Specifically, we focus on *Drosophila* larval brain type II NB (NBII) lineages (Figure 4A).[22,93,94] NBII lineages divide asymmetrically to give rise to another NB and, instead of a GMC, like in NBI lineages, an intermediate neural progenitor (INP) (Figure 4A; see also Figure 1A). This INP will divide asymmetrically to give rise to another INP and a GMC (Figure 4A). Hence, given this extra intermediate phase of proliferation, the NBII lineages are larger and more prone than NBI lineages to induce tumor-like overgrowth when the ASCD process fails.[22] In a normal NBII lineage, only one NB is present, expressing the transcription factor Deadpan (Dpn), as well as several INPs, expressing both Dpn and the transcription factor Asense (Ase) (Figures 4A and 4B). In $p53^{E8}$ null mutant NBII clones, we did not observe any overgrowth of the clone or even the presence of ectopic NBs (Dpn^{+} Ase^{-}) (Figure 4B). Intriguingly, the localization of Numb in NBII lineage dividing cells (i.e., NBs and INPs) was not significantly altered either (Figure S3A). In a similar way, the larval brain NBI lineages, which are comparable to the embryonic NBI lineages, did not show significant failures in Numb localization in mitotic cells or ectopic NBs after downregulating *p53* in these lineages (Figures S3B and S3C). One possibility to explain these results is that there are enough levels of Numb in the quiescent larval NBs before they resume division at late first/early second instar larval stage. This, along with the high redundancy in ASCD regulation to ensure the basal presence of cell-fate determinants, may contribute to explain this lack of overgrowth in larval *p53* mutant NB clones[95,96] (see also discussion). Hence, we decided to analyze the *p53* mutant phenotype in a sensitized genetic background in which the ASCD process is altered but does not yet induce tumor-like overgrowth.[97] This sensitized genetic background consisted in the overexpression of a constitutively activated form of *Ras* (Ras^{V12}) plus the complete loss of the ASCD regulator and tumor suppressor gene *scribble* (*scrib*).[97] However, we did not observe tumor-like overgrowth or any qualitative increase in the phenotype of Ras^{V12} $scrib^{2}$ after downregulating *p53* in the Ras^{V12} $scrib^{2}$ genetic background. Even more, the Ras^{V12} $scrib^{2}$ ectopic NB phenotype was partially suppressed after downregulating *p53* (Figure 4C). Thus, *p53* loss might be interacting with other ASCD regulator genes in NBII lineages to be able to cause tumoral overgrowth when they fail simultaneously (see also discussion).

DISCUSSION

p53 is one of the most relevant tumor suppressor genes, as it is mutated in about 50% of all human tumors. Apart from the extensively studied canonical functions of p53, additional non-canonical processes modulated by p53 have been unveiled over the past years, including the mode of stem cell division regulation. However, the mechanisms by which p53 is modulating this process remain elusive.[43,56,60] Given that p53 is a transcription factor, we hypothesized that p53 might be directly regulating the expression levels of ASCD regulators. Interestingly, some among the 86 direct p53 target genes commonly predicted in mice and humans in a recent *in silico* study, such as *TRIM32* and *TRAF4*, related or even orthologue of *Drosophila* ASCD regulators Brat and Traf4, respectively.[73] We were

Table 2. Primers used for the ChIP experiments

Gene	Fw primer	Rev primer
3′UTR	GTGGCAGCCGGTCGAA	CAGCCAAAGCGGATGCA
p53PROM	CGCTTGTACTTGCATCATTCG	GCGCCTTGGCTGGATAAAC
brat	GAATGGTTCCGTGGTTCGTTG	AACAATTACGCCAAGCGTTGA
Traf4	GTGCAAAGGAGAGGGGTTAC	ACGCCAATTCCTTGGAGCCAG
numb	ACCGAGACAAGCTCGATTGG	ATTACCCCTCTTTTGGCGGG

aware that the mechanisms by which ASCD regulators operate, or at least those that have been predominantly described, relay mainly on protein-protein interactions and post-translational modifications, largely phosphorylation events. However, the relevance of ASCD regulation at the transcriptional level is coming on stage over the past years.[98–104] In this work, we have found that *Drosophila* p53 is, in fact, modulating ASCD by directly regulating the expression of key ASCD regulators: Numb, Brat, and Traf4.

Numb action has been traditionally associated to the inhibition of the transmembrane Notch receptor and the consequent induction of differentiation in the daughter cell in which is asymmetrically segregated, as it has been shown in *Drosophila* nervous system, in mammals and in human carcinogenesis.[105–108] Remarkably, the tumor suppressor effect of human NUMB has also been linked to its capacity to stabilize p53 in human mammary gland, preventing the MDM2-mediated ubiquitination and consequent p53 degradation.[109] Likewise, Numb, in mouse mammary epithelial stem cells, ensures high p53 activity in the cell in which it is asymmetrically segregated, and the loss of Numb promotes *p53* loss-of-function-induced tumorigenesis.[110] Intriguingly, here we have found that *Drosophila* p53 directly activates the expression of Numb. Thus, it would be interesting to analyze whether this is also the case in mammals. The establishment of such positive feedback loop could reinforce the regulatory function of the Numb-p53 pathway.[111] That could also explain, at least in part, the mechanism by which p53 favors an asymmetric mode of cell division in isolated human mammary stem cells.[3]

Drosophila TRIM-NHL protein Brat is related to human TRIM proteins (TRIM2, TRIM3, and TRIM32), especially closer to TRIM3, a tumor suppressor gene also involved in regulating ASCD.[7] Curiously, the role of human TRIM32 seems to be cell type and context dependent. For example, TRIM32, identified as a novel p53 target some years ago, in turn binds and degrades p53 by ubiquitination,[112] suggesting a tumorigenic effect of TRIM32. However, TRIM32 has also been demonstrated to induce ASCD in neuroblastoma cells and other progenitor cells, behaving as a tumor suppressor gene.[113–115] A similar effect has been observed in mouse TRIM32, which prevents self-renewal in neural progenitors, promoting differentiation through microRNAs.[116]

The function of human TRAF4 in the context of ASCD has not been reported. It has been described that the expression levels of TRAF4 are elevated in many human cancers, normally associated with gene amplification.[117,118] *In vivo* experiments in mouse also suggest an oncogenic role for TRAF4.[119] Thus, in the case of TRAF4, a potential tumor suppressor role in particular contexts or cell types is not yet clear.

Despite finding that *Drosophila* p53 was regulating crucial ASCD effectors, such as the cell-fate determinants Numb and Brat, the loss of *p53* did not cause tumor-like overgrowth in larval brain NB lineages. One potential explanation for this result is the high redundancy in the regulation of the ASCD process to basally localize those cell-fate determinants. The loss of cell-fate determinants, particularly *numb* or *brat*, has been reported to cause tumor-like overgrowth.[22,120] However, mutations in the components of the apical complex or other ASCD regulators that modulate the basal localization of those cell-fate determinants does not normally cause tumoral growth.[95,96] In fact, we have previously found that the loss of at least two of these latter ASCD regulators is required to provoke tumor-like overgrowth.[95–97] Thus, we hypothesize that p53 might be functionally interacting with other ASCD regulators to activate Numb, Brat, and Traf4. In the absence of p53, those regulators might be compensating the loss of p53, avoiding stronger phenotypes. Actually, even though the loss of *p53* caused significant defects in the localization of Numb and Brat in the embryonic metaphase NBs, the phenotype was not completely penetrant, and both determinants were still found in a percent of the *p53* null mutant metaphase NBs (Figure 2). Moreover, that phenotype seemed to be at least partially suppressed during telophase (Figure S1). These compensatory or redundant mechanisms in the ASCD regulation process might also help to understand why *p53* null mutants can even reach the adulthood. However, as we observed, the viability of *p53* null mutants is compromised throughout the life cycle, suggesting that these mutants are more sensitive to any potential genetic change/mutation that could unveil stronger phenotypes.

A plausible explanation to justify the lack of synergism between *p53* loss and Ras^{V12} $scrib^{2}$ (Figure 4C) is the molecular loop defined between p53 and Ras, in which the loss of *p53* implies the activation of the Ras signaling cascade, placing them in the same pathway.[121,122] However, the partial suppression of the Ras^{V12} $scrib^{2}$ phenotype after downregulating *p53* in NB clones (Figure 4C) suggests that the loss of *p53* in this context is affecting, directly or indirectly, other unknown factors/signaling pathways relevant for the correct development of NB lineages. In fact, the effects, autonomous and non-autonomous, of p53 in different organisms and environments are complex and involve diverse and multiple targets, which are even different in normal and acute cell stress conditions.[43,56,59,123,124] Thus, it would be intriguing but challenging to search in the future for those ASCD regulators whose loss synergistically interact with the loss of *p53* to induce tumor-like overgrowth.

Given the conservation of the *Drosophila* genes *numb*, *brat*, and *Traf4* in humans and mice, it would be appealing to validate *in vivo* whether TP53/Trp53 also modulates the mode of stem cell division, promoting differentiation, by directly impinging on the mammalian

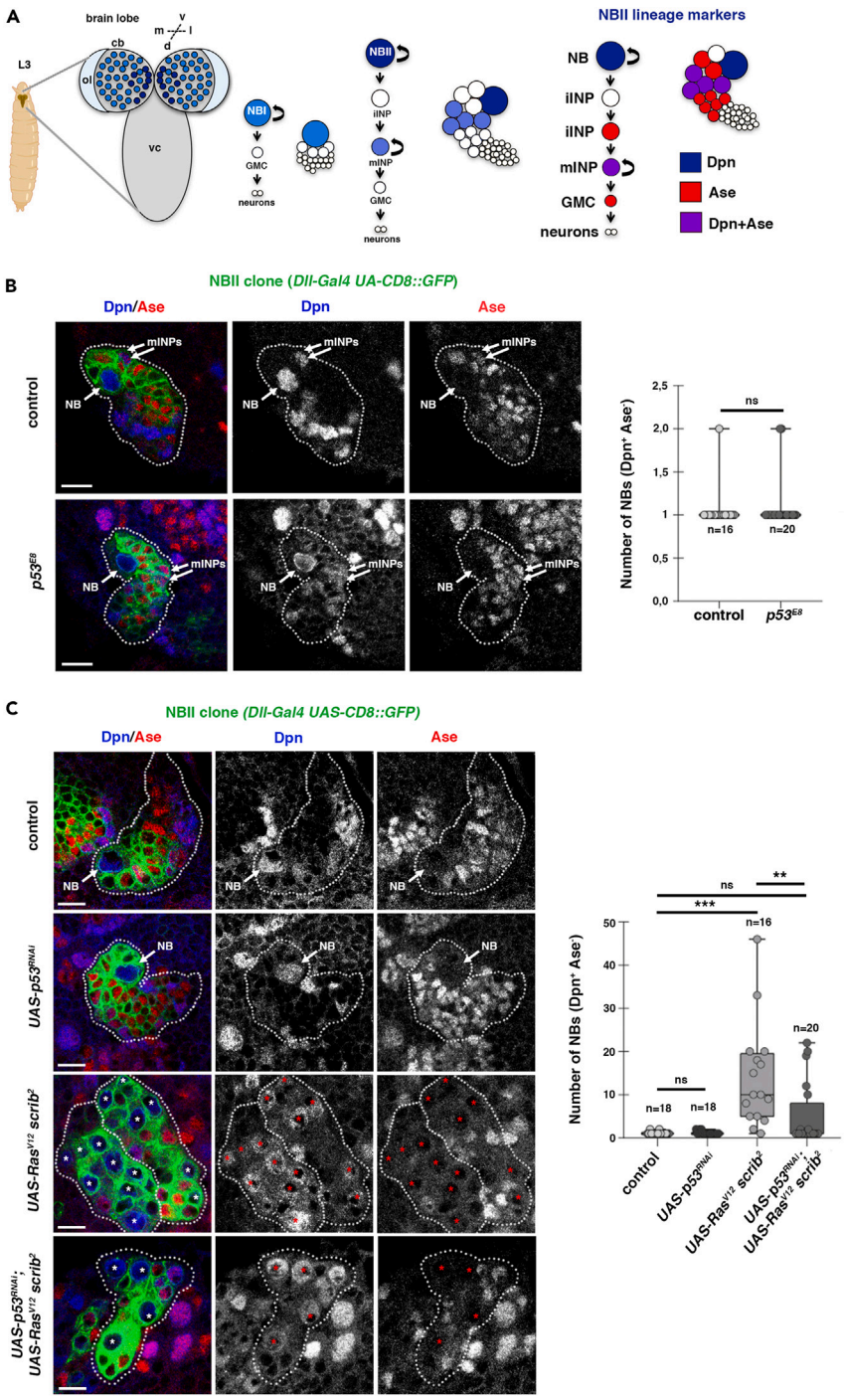

Figure 4. *p53* loss does not induce tumor-like overgrowth in larval brain NB lineages

(A) The *Drosophila* larval central brain (cb) contains type I (NBI) and type II (NBII) NBs. L3, third instar larva; ol, optic lobe; vc, ventral cord; m, medial; l, lateral; d, dorsal; v, ventral; iINP, immature INP; mIPN, mature INP.

(B) Confocal immunofluorescences showing an NBII lineage. *p53* loss does not induce tumorigenesis or even a significant number of ectopic NBs within NBII lineages. Data are represented as medians within the interquartile range (box) and the maximum and minimum values (whiskers); n = number of NB lineages analyzed. A Mann-Whitney test was used (ns, not significant in the boxplots).

(C) Confocal immunofluorescences showing an NBII lineage. *p53* downregulation partially suppressed the *UAS-Ras^{V12} scrib^{2}* ectopic NB phenotype. Data are represented as medians within the interquartile range (box) and the maximum and minimum values (whiskers); n = number of NB lineages analyzed. A Kruskal-Wallis test was used (ns, not significant; $^{**}p < 0.01$, $^{***}p < 0.001$ in the boxplots). Scale bar: 10 μm. See also Figure S3.

closest homologues of these *Drosophila* ASCD target genes. This could impact our understanding of the high complexity of p53 pleiotropic effects to achieve its tumor suppressor activity.

Limitations of the study

In this work, we have found that *Drosophila* p53 tumor suppressor and transcription factor is regulating the process of ASCD in NBs. Furthermore, we have shown that p53 is directly activating key ASCD modulator genes, such as those that encode the apical protein Traf4 and the cell fate determinants Brat and Numb. However, despite of that, we have not detected any tumor-like overgrowth in the *Drosophila* larval brain NB lineages mutant for *p53*. We hypothesize that p53 might be functionally interacting with other ASCD regulators to activate *numb*, *brat*, and *Traf4*. Hence, in the absence of p53, those regulators might be compensating the loss of p53, avoiding stronger phenotypes. One challenging aim in the future will be looking for those ASCD regulators whose loss synergistically interacts with the loss of p53 to induce tumor-like overgrowth.

RESOURCE AVAILABILITY

Lead contact

Further information and requests for resources and reagents should be directed to and will be fulfilled by the lead contact, Ana Carmena (acarmena@umh.es).

Materials availability

This study did not generate new unique reagents.

Data and code availability

- Original data reported in this paper will be shared by the lead contact upon request.
- This paper does not report original code.
- Any additional information required to reanalyze the date reported in this paper is available from the lead contact upon request.

ACKNOWLEDGMENTS

We thank J. Chung, J. Knoblich, A. Wodarz, the Bloomington *Drosophila* Stock Center at the University of Indiana, and the Developmental Studies Hybridoma Bank at the University of Iowa for kindly providing fly strains and reagents. This work was supported by the Spanish grants from the Ministry of Economy and Competitiveness (BFU2015-64251), the Ministry of Science, Innovation and Universities (PGC2018-097093-B-100), the Ministry of Science and Innovation (PID2021-123196NB-100), the Generalitat Valenciana Prometeo/2021/052 grant, and by FEDER (European Regional Development Fund). S.M.-O. was supported by a predoctoral FPI fellowship associated to the BFU2015-64251 grant. The "Instituto de Neurociencias" in Alicante is a "Severo Ochoa Center of Excellence in R&D." Our group belongs to "Conexión Cáncer" (CSIC).

AUTHOR CONTRIBUTIONS

S.M.-O. conducted experiments and analyzed the data; M.F. conducted experiments and analyzed the data; M.L. conducted experiments; A.C. conceived the study, designed the experiments, analyzed data, and wrote the manuscript.

DECLARATION OF INTERESTS

The authors declare no competing interests.

STAR★METHODS

Detailed methods are provided in the online version of this paper and include the following:

- KEY RESOURCES TABLE
- EXPERIMENTAL MODEL AND STUDY PARTICIPANT DETAILS
  - *Drosophila* strains and genetics
  - Drosophila husbandry
- METHOD DETAILS
  - Immunohistochemistry, immunofluorescence and microscopy
  - MARCM clones
  - qRTPCR
  - ChIP experiments
  - ChIPseq data processing and visualization
- QUANTIFICATION AND STATISTICAL ANALYSIS

SUPPLEMENTAL INFORMATION

Supplemental information can be found online at https://doi.org/10.1016/j.isci.2024.111118.

Received: March 3, 2024
Revised: August 8, 2024
Accepted: October 3, 2024
Published: October 9, 2024

REFERENCES

1. Knoblich, J.A. (2010). Asymmetric cell division: recent developments and their implications for tumour biology. Nat. Rev. Mol. Cell Biol. *11*, 849–860. https://doi.org/10.1038/nrm3010.
2. Sugiarto, S., Persson, A.I., Munoz, E.G., Waldhuber, M., Lamagna, C., Andor, N., Hanecker, P., Ayers-Ringler, J., Phillips, J., Siu, J., et al. (2011). Asymmetry-defective oligodendrocyte progenitors are glioma precursors. Cancer Cell *20*, 328–340. https://doi.org/10.1016/j.ccr.2011.08.011.
3. Cicalese, A., Bonizzi, G., Pasi, C.E., Faretta, M., Ronzoni, S., Giulini, B., Brisken, C., Minucci, S., Di Fiore, P.P., and Pelicci, P.G. (2009). The tumor suppressor p53 regulates polarity of self-renewing divisions in mammary stem cells. Cell *138*, 1083–1095. https://doi.org/10.1016/j.cell.2009.06.048.
4. Bu, P., Chen, K.Y., Chen, J.H., Wang, L., Walters, J., Shin, Y.J., Goerger, J.P., Sun, J., Witherspoon, M., Rakhilin, N., et al. (2013). A microRNA miR-34a-regulated bimodal switch targets Notch in colon cancer stem cells. Cell Stem Cell *12*, 602–615. https://doi.org/10.1016/j.stem.2013.03.002.
5. Hwang, W.L., Jiang, J.K., Yang, S.H., Huang, T.S., Lan, H.Y., Teng, H.W., Yang, C.Y., Tsai, Y.P., Lin, C.H., Wang, H.W., and Yang, M.H. (2014). MicroRNA-146a directs the symmetric division of Snail-dominant colorectal cancer stem cells. Nat. Cell Biol. *16*, 268–280. https://doi.org/10.1038/ncb2910.
6. Daynac, M., Chouchane, M., Collins, H.Y., Murphy, N.E., Andor, N., Niu, J., Fancy, S.P.J., Stallcup, W.B., and Petritsch, C.K. (2018). Lgl1 controls NG2 endocytic pathway to regulate oligodendrocyte differentiation and asymmetric cell division and gliomagenesis. Nat. Commun. *9*, 2862. https://doi.org/10.1038/s41467-018-05099-3.
7. Chen, G., Kong, J., Tucker-Burden, C., Anand, M., Rong, Y., Rahman, F., Moreno, C.S., Van Meir, E.G., Hadjipanayis, C.G., and Brat, D.J. (2014). Human Brat ortholog TRIM3 is a tumor suppressor that regulates asymmetric cell division in glioblastoma. Cancer Res. *74*, 4536–4548. https://doi.org/10.1158/0008-5472.CAN-13-3703.
8. Gómez-López, S., Lerner, R.G., and Petritsch, C. (2014). Asymmetric cell division of stem and progenitor cells during homeostasis and cancer. Cell. Mol. Life Sci. *71*, 575–597. https://doi.org/10.1007/s00018-013-1386-1.
9. Samanta, P., Bhowmik, A., Biswas, S., Sarkar, R., Ghosh, R., Pakhira, S., Mondal, M., Sen, S., Saha, P., and Hajra, S. (2023). Therapeutic Effectiveness of Anticancer Agents Targeting Different Signaling Molecules Involved in Asymmetric Division of Cancer Stem Cell. Stem Cell Rev. Rep. *19*, 1283–1306. https://doi.org/10.1007/s12015-023-10523-3.
10. Homem, C.C.F., and Knoblich, J.A. (2012). Drosophila neuroblasts: a model for stem cell biology. Development *139*, 4297–4310. https://doi.org/10.1242/dev.080515.
11. Gallaud, E., Pham, T., and Cabernard, C. (2017). Drosophila melanogaster Neuroblasts: A Model for Asymmetric Stem Cell Divisions. Results Probl. Cell Differ. *61*, 183–210. https://doi.org/10.1007/978-3-319-53150-2_8.
12. Knoblich, J.A. (2008). Mechanisms of asymmetric stem cell division. Cell *132*, 583–597. https://doi.org/10.1016/j.cell.2008.02.007.
13. Petronczki, M., and Knoblich, J.A. (2001). DmPAR-6 directs epithelial polarity and asymmetric cell division of neuroblasts in Drosophila. Nat. Cell Biol. *3*, 43–49. https://doi.org/10.1038/35050550.
14. Schober, M., Schaefer, M., and Knoblich, J.A. (1999). Bazooka recruits Inscuteable to orient asymmetric cell divisions in Drosophila neuroblasts. Nature *402*, 548–551. https://doi.org/10.1038/990135.
15. Wodarz, A., Ramrath, A., Grimm, A., and Knust, E. (2000). Drosophila atypical protein kinase C associates with Bazooka and controls polarity of epithelia and neuroblasts. J. Cell Biol. *150*, 1361–1374. https://doi.org/10.1083/jcb.150.6.1361.
16. Wodarz, A., Ramrath, A., Kuchinke, U., and Knust, E. (1999). Bazooka provides an apical cue for Inscuteable localization in Drosophila neuroblasts. Nature *402*, 544–547. https://doi.org/10.1038/990128.
17. de Torres-Jurado, A., Manzanero-Ortiz, S., and Carmena, A. (2022). Glial-secreted Netrins regulate Robo1/Rac1-Cdc42 signaling threshold levels during Drosophila asymmetric neural stem/progenitor cell division. Curr. Biol. *32*, 2174–2188.e3. https://doi.org/10.1016/j.cub.2022.04.001.
18. Carmena, A., Makarova, A., and Speicher, S. (2011). The Rap1-Rgl-Ral signaling network regulates neuroblast cortical polarity and spindle orientation. J. Cell Biol. *195*, 553–562. https://doi.org/10.1083/jcb.201108112.
19. Atwood, S.X., Chabu, C., Penkert, R.R., Doe, C.Q., and Prehoda, K.E. (2007). Cdc42 acts downstream of Bazooka to regulate neuroblast polarity through Par-6 aPKC. J. Cell Sci. *120*, 3200–3206. https://doi.org/10.1242/jcs.014902.
20. Bello, B., Reichert, H., and Hirth, F. (2006). The brain tumor gene negatively regulates neural progenitor cell proliferation in the larval central brain of Drosophila. Development *133*, 2639–2648. https://doi.org/10.1242/dev.02429.
21. Betschinger, J., Mechtler, K., and Knoblich, J.A. (2006). Asymmetric segregation of the tumor suppressor brat regulates self-renewal in Drosophila neural stem cells. Cell *124*, 1241–1253.
22. Bowman, S.K., Rolland, V., Betschinger, J., Kinsey, K.A., Emery, G., and Knoblich, J.A. (2008). The tumor suppressors Brat and Numb regulate transit-amplifying neuroblast lineages in Drosophila. Dev. Cell *14*, 535–546. https://doi.org/10.1016/j.devcel.2008.03.004.
23. Lee, C.Y., Wilkinson, B.D., Siegrist, S.E., Wharton, R.P., and Doe, C.Q. (2006). Brat is a Miranda cargo protein that promotes neuronal differentiation and inhibits neuroblast self-renewal. Dev. Cell *10*, 441–449.
24. Knoblich, J.A., Jan, L.Y., and Jan, Y.N. (1995). Asymmetric segregation of Numb and Prospero during cell division. Nature *377*, 624–627. https://doi.org/10.1038/377624a0.
25. Uemura, T., Shepherd, S., Ackerman, L., Jan, L.Y., and Jan, Y.N. (1989). numb, a gene required in determination of cell fate during sensory organ formation in Drosophila embryos. Cell *58*, 349–360. https://doi.org/10.1016/0092-8674(89)90849-0.
26. Rhyu, M.S., Jan, L.Y., and Jan, Y.N. (1994). Asymmetric distribution of numb protein during division of the sensory organ precursor cell confers distinct fates to daughter cells. Cell *76*, 477–491. https://doi.org/10.1016/0092-8674(94)90112-0.
27. Smith, C.A., Lau, K.M., Rahmani, Z., Dho, S.E., Brothers, G., She, Y.M., Berry, D.M., Bonneil, E., Thibault, P., Schweisguth, F., et al. (2007). aPKC-mediated phosphorylation regulates asymmetric membrane localization of the cell fate determinant Numb. EMBO J. *26*, 468–480. https://doi.org/10.1038/sj.emboj.7601495.
28. Caussinus, E., and Gonzalez, C. (2005). Induction of tumor growth by altered stem-cell asymmetric division in Drosophila melanogaster. Nat. Genet. *37*, 1125–1129. https://doi.org/10.1038/ng1632.
29. Albertson, R., and Doe, C.Q. (2003). Dlg, Scrib and Lgl regulate neuroblast cell size and mitotic spindle asymmetry. Nat. Cell Biol. *5*, 166–170. https://doi.org/10.1038/ncb922.
30. Ohshiro, T., Yagami, T., Zhang, C., and Matsuzaki, F. (2000). Role of cortical tumour-suppressor proteins in asymmetric division of Drosophila neuroblast. Nature *408*, 593–596. https://doi.org/10.1038/35046087.
31. Peng, C.Y., Manning, L., Albertson, R., and Doe, C.Q. (2000). The tumour-suppressor genes lgl and dlg regulate basal protein targeting in Drosophila neuroblasts. Nature *408*, 596–600.
32. Gateff, E.a.S. (1967). Developmental studies of a new mutant of Drosophila melanogaster: Lethal malignant brain tumor (l(2)gl 4). Am. Zool. *7*.
33. Gateff, E., and Schneiderman, H.A. (1969). Neoplasms in mutant and cultured wild-tupe tissues of Drosophila. Natl. Cancer Inst. Monogr. *31*, 365–397.
34. Gateff, E., and Schneiderman, H.A. (1974). Developmental capacities of benign and malignant neoplasms of Drosophila. Wilhelm Roux Arch. Entwickl. Mech. Org. *176*, 23–65. https://doi.org/10.1007/BF00577830.
35. Gateff, E. (1978). Malignant neoplasms of genetic origin in Drosophila melanogaster. Science *200*, 1448–1459.
36. Bouaoun, L., Sonkin, D., Ardin, M., Hollstein, M., Byrnes, G., Zavadil, J., and Olivier, M. (2016). TP53 Variations in Human Cancers: New Lessons from the IARC TP53 Database and Genomics Data. Hum. Mutat. *37*, 865–876. https://doi.org/10.1002/humu.23035.
37. Vousden, K.H., and Prives, C. (2009). Blinded by the Light: The Growing Complexity of p53. Cell *137*, 413–431. https://doi.org/10.1016/j.cell.2009.04.037.
38. Kandoth, C., McLellan, M.D., Vandin, F., Ye, K., Niu, B., Lu, C., Xie, M., Zhang, Q., McMichael, J.F., Wyczalkowski, M.A., et al. (2013). Mutational landscape and significance across 12 major cancer types. Nature *502*, 333–339. https://doi.org/10.1038/nature12634.
39. Lane, D.P. (1992). Cancer. p53, guardian of the genome. Nature *358*, 15–16. https://doi.org/10.1038/358015a0.
40. Muller, P.A.J., and Vousden, K.H. (2013). p53 mutations in cancer. Nat. Cell Biol. *15*, 2–8. https://doi.org/10.1038/ncb2641.

41. Zhang, Y., and Lozano, G. (2017). p53: Multiple Facets of a Rubik's Cube. Annu. Rev. Cell Biol. *1*, 185–201. https://doi.org/10.1146/annurev-cancerbio-050216-121926.
42. Pant, V., and Lozano, G. (2014). Limiting the power of p53 through the ubiquitin proteasome pathway. Genes Dev. *28*, 1739–1751. https://doi.org/10.1101/gad.247452.114.
43. Boutelle, A.M., and Attardi, L.D. (2021). p53 and Tumor Suppression: It Takes a Network. Trends Cell Biol. *31*, 298–310. https://doi.org/10.1016/j.tcb.2020.12.011.
44. Hernández Borrero, L.J., and El-Deiry, W.S. (2021). Tumor suppressor p53: Biology, signaling pathways, and therapeutic targeting. Biochim. Biophys. Acta Rev. Canc *1876*, 188556. https://doi.org/10.1016/j.bbcan.2021.188556.
45. Marei, H.E., Althani, A., Afifi, N., Hasan, A., Caceci, T., Pozzoli, G., Morrione, A., Giordano, A., and Cenciarelli, C. (2021). p53 signaling in cancer progression and therapy. Cancer Cell Int. *21*, 703. https://doi.org/10.1186/s12935-021-02396-8.
46. Kress, M., May, E., Cassingena, R., and May, P. (1979). Simian virus 40-transformed cells express new species of proteins precipitable by anti-simian virus 40 tumor serum. J. Virol. *31*, 472–483. https://doi.org/10.1128/JVI.31.2.472-483.1979.
47. Lane, D.P., and Crawford, L.V. (1979). T antigen is bound to a host protein in SV40-transformed cells. Nature *278*, 261–263. https://doi.org/10.1038/278261a0.
48. Linzer, D.I., and Levine, A.J. (1979). Characterization of a 54K dalton cellular SV40 tumor antigen present in SV40-transformed cells and uninfected embryonal carcinoma cells. Cell *17*, 43–52. https://doi.org/10.1016/0092-8674(79)90293-9.
49. Melero, J.A., Stitt, D.T., Mangel, W.F., and Carroll, R.B. (1979). Identification of new polypeptide species (48-55K) immunoprecipitable by antiserum to purified large T antigen and present in SV40-infected and -transformed cells. Virology *93*, 466–480. https://doi.org/10.1016/0042-6822(79)90250-2.
50. Smith, A.E., Smith, R., and Paucha, E. (1979). Characterization of different tumor antigens present in cells transformed by simian virus 40. Cell *18*, 335–346. https://doi.org/10.1016/0092-8674(79)90053-9.
51. Tyner, S.D., Venkatachalam, S., Choi, J., Jones, S., Ghebranious, N., Igelmann, H., Lu, X., Soron, G., Cooper, B., Brayton, C., et al. (2002). p53 mutant mice that display early ageing-associated phenotypes. Nature *415*, 45–53. https://doi.org/10.1038/415045a.
52. Van Nostrand, J.L., Brady, C.A., Jung, H., Fuentes, D.R., Kozak, M.M., Johnson, T.M., Lin, C.Y., Lin, C.J., Swiderski, D.L., Vogel, H., et al. (2014). Inappropriate p53 activation during development induces features of CHARGE syndrome. Nature *514*, 228–232. https://doi.org/10.1038/nature13585.
53. McGowan, K.A., Li, J.Z., Park, C.Y., Beaudry, V., Tabor, H.K., Sabnis, A.J., Zhang, W., Fuchs, H., de Angelis, M.H., Myers, R.M., et al. (2008). Ribosomal mutations cause p53-mediated dark skin and pleiotropic effects. Nat. Genet. *40*, 963–970. https://doi.org/10.1038/ng.188.
54. Levine, A.J., and Berger, S.L. (2017). The interplay between epigenetic changes and the p53 protein in stem cells. Genes Dev. *31*, 1195–1201. https://doi.org/10.1101/gad.298984.117.
55. Cooks, T., Harris, C.C., and Oren, M. (2014). Caught in the cross fire: p53 in inflammation. Carcinogenesis *35*, 1680–1690. https://doi.org/10.1093/carcin/bgu134.
56. Jain, A.K., and Barton, M.C. (2018). p53: emerging roles in stem cells, development and beyond. Development *145*, dev158360. https://doi.org/10.1242/dev.158360.
57. Aylon, Y., and Oren, M. (2016). The Paradox of p53: What, How, and Why? Cold Spring Harb. Perspect. Med. *6*, a026328. https://doi.org/10.1101/cshperspect.a026328.
58. Ingaramo, M.C., Sánchez, J.A., and Dekanty, A. (2018). Regulation and function of p53: A perspective from Drosophila studies. Mech. Dev. *154*, 82–90. https://doi.org/10.1016/j.mod.2018.05.007.
59. Pappas, K., Xu, J., Zairis, S., Resnick-Silverman, L., Abate, F., Steinbach, N., Ozturk, S., Saal, L.H., Su, T., Cheung, P., et al. (2017). p53 Maintains Baseline Expression of Multiple Tumor Suppressor Genes. Mol. Cancer Res. *15*, 1051–1062. https://doi.org/10.1158/1541-7786.MCR-17-0089.
60. Spike, B.T., and Wahl, G.M. (2011). p53, Stem Cells, and Reprogramming: Tumor Suppression beyond Guarding the Genome. Genes Cancer *2*, 404–419. https://doi.org/10.1177/1947601911410224.
61. Ouadah, Y., Rojas, E.R., Riordan, D.P., Capostagno, S., Kuo, C.S., and Krasnow, M.A. (2019). Rare Pulmonary Neuroendocrine Cells Are Stem Cells Regulated by Rb, p53, and Notch. Cell *179*, 403–416.e23. https://doi.org/10.1016/j.cell.2019.09.010.
62. Jin, S., Martinek, S., Joo, W.S., Wortman, J.R., Mirkovic, N., Sali, A., Yandell, M.D., Pavletich, N.P., Young, M.W., and Levine, A.J. (2000). Identification and characterization of a p53 homologue in Drosophila melanogaster. Proc. Natl. Acad. Sci. USA *97*, 7301–7306. https://doi.org/10.1073/pnas.97.13.7301.
63. Ollmann, M., Young, L.M., Di Como, C.J., Karim, F., Belvin, M., Robertson, S., Whittaker, K., Demsky, M., Fisher, W.W., Buchman, A., et al. (2000). Drosophila p53 is a structural and functional homolog of the tumor suppressor p53. Cell *101*, 91–101. https://doi.org/10.1016/S0092-8674(00)80626-1.
64. Brodsky, M.H., Weinert, B.T., Tsang, G., Rong, Y.S., McGinnis, N.M., Golic, K.G., Rio, D.C., and Rubin, G.M. (2004). Drosophila melanogaster MNK/Chk2 and p53 regulate multiple DNA repair and apoptotic pathways following DNA damage. Mol. Cell Biol. *24*, 1219–1231. https://doi.org/10.1128/MCB.24.3.1219-1231.2004.
65. Sogame, N., Kim, M., and Abrams, J.M. (2003). Drosophila p53 preserves genomic stability by regulating cell death. Proc. Natl. Acad. Sci. USA *100*, 4696–4701. https://doi.org/10.1073/pnas.0736384100.
66. Mandal, S., Freije, W.A., Guptan, P., and Banerjee, U. (2010). Metabolic control of G1-S transition: cyclin E degradation by p53-induced activation of the ubiquitin-proteasome system. J. Cell Biol. *188*, 473–479. https://doi.org/10.1083/jcb.200912024.
67. Yamasaki, S., Yagishita, N., Sasaki, T., Nakazawa, M., Kato, Y., Yamadera, T., Bae, E., Toriyama, S., Ikeda, R., Zhang, L., et al. (2007). Cytoplasmic destruction of p53 by the endoplasmic reticulum-resident ubiquitin ligase 'Synoviolin'. EMBO J. *26*, 113–122. https://doi.org/10.1038/sj.emboj.7601490.
68. Chakraborty, R., Li, Y., Zhou, L., and Golic, K.G. (2015). Corp Regulates P53 in Drosophila melanogaster via a Negative Feedback Loop. PLoS Genet. *11*, e1005400. https://doi.org/10.1371/journal.pgen.1005400.
69. de la Cova, C., Senoo-Matsuda, N., Ziosi, M., Wu, D.C., Bellosta, P., Quinzii, C.M., and Johnston, L.A. (2014). Supercompetitor status of Drosophila Myc cells requires p53 as a fitness sensor to reprogram metabolism and promote viability. Cell Metabol. *19*, 470–483. https://doi.org/10.1016/j.cmet.2014.01.012.
70. Mesquita, D., Dekanty, A., and Milán, M. (2010). A dp53-dependent mechanism involved in coordinating tissue growth in Drosophila. PLoS Biol. *8*, e1000566. https://doi.org/10.1371/journal.pbio.1000566.
71. Barrio, L., Dekanty, A., and Milán, M. (2014). MicroRNA-mediated regulation of Dp53 in the Drosophila fat body contributes to metabolic adaptation to nutrient deprivation. Cell Rep. *8*, 528–541. https://doi.org/10.1016/j.celrep.2014.06.020.
72. Herzog, G., Joerger, A.C., Shmueli, M.D., Fersht, A.R., Gazit, E., and Segal, D. (2012). Evaluating Drosophila p53 as a model system for studying cancer mutations. J. Biol. Chem. *287*, 44330–44337. https://doi.org/10.1074/jbc.M112.417980.
73. Fischer, M. (2019). Conservation and divergence of the p53 gene regulatory network between mice and humans. Oncogene *38*, 4095–4109. https://doi.org/10.1038/s41388-019-0706-9.
74. Lee, J.H., Lee, E., Park, J., Kim, E., Kim, J., and Chung, J. (2003). In vivo p53 function is indispensable for DNA damage-induced apoptotic signaling in Drosophila. FEBS Lett. *550*, 5–10. https://doi.org/10.1016/s0014-5793(03)00771-3.
75. Chu-LaGraff, Q., and Doe, C.Q. (1993). Neuroblast specification and formation regulated by wingless in the Drosophila CNS. Science *261*, 1594–1597. https://doi.org/10.1126/science.8372355.
76. Bhat, K.M., and Schedl, P. (1994). The Drosophila miti-mere gene, a member of the POU family, is required for the specification of the RP2/sibling lineage during neurogenesis. Development *120*, 1483–1501. https://doi.org/10.1242/dev.120.6.1483.
77. Bossing, T., Udolph, G., Doe, C.Q., and Technau, G.M. (1996). The embryonic central nervous system lineages of Drosophila melanogaster. I. Neuroblast lineages derived from the ventral half of the neuroectoderm. Dev. Biol. *179*, 41–64. https://doi.org/10.1006/dbio.1996.0240.
78. Buescher, M., Yeo, S.L., Udolph, G., Zavortink, M., Yang, X., Tear, G., and Chia, W. (1998). Binary sibling neuronal cell fate decisions in the Drosophila embryonic central nervous system are nonstochastic and require inscuteable-mediated asymmetry of ganglion mother cells. Genes Dev. *12*, 1858–1870. https://doi.org/10.1101/gad.12.12.1858.
79. Skeath, J.B., and Doe, C.Q. (1998). Sanpodo and Notch act in opposition to Numb to distinguish sibling neuron fates in the Drosophila CNS. Development *125*,

1857–1865. https://doi.org/10.1242/dev.125.10.1857.
80. Bhat, K.M., Gaziova, I., and Katipalla, S. (2011). Neuralized mediates asymmetric division of neural precursors by two distinct and sequential events: promoting asymmetric localization of Numb and enhancing activation of Notch-signaling. Dev. Biol. *351*, 186–198. https://doi.org/10.1016/j.ydbio.2010.12.008.
81. Speicher, S., Fischer, A., Knoblich, J., and Carmena, A. (2008). The PDZ protein Canoe regulates the asymmetric division of Drosophila neuroblasts and muscle progenitors. Curr. Biol. *18*, 831–837. https://doi.org/10.1016/j.cub.2008.04.072.
82. Keder, A., Rives-Quinto, N., Aerne, B.L., Franco, M., Tapon, N., and Carmena, A. (2015). The hippo pathway core cassette regulates asymmetric cell division. Curr. Biol. *25*, 2739–2750. https://doi.org/10.1016/j.cub.2015.08.064.
83. Wang, H., Cai, Y., Chia, W., and Yang, X. (2006). Drosophila homologs of mammalian TNF/TNFR-related molecules regulate segregation of Miranda/Prospero in neuroblasts. EMBO J. *25*, 5783–5793. https://doi.org/10.1038/sj.emboj.7601461.
84. Senitzki, A., Safieh, J., Sharma, V., Golovenko, D., Danin-Poleg, Y., Inga, A., and Haran, T.E. (2021). The complex architecture of p53 binding sites. Nucleic Acids Res. *49*, 1364–1382. https://doi.org/10.1093/nar/gkaa1283.
85. Wang, B., Xiao, Z., and Ren, E.C. (2009). Redefining the p53 response element. Proc. Natl. Acad. Sci. USA *106*, 14373–14378. https://doi.org/10.1073/pnas.0903284106.
86. Yan, J., Menendez, D., Yang, X.P., Resnick, M.A., and Jetten, A.M. (2009). A regulatory loop composed of RAP80-HDM2-p53 provides RAP80-enhanced p53 degradation by HDM2 in response to DNA damage. J. Biol. Chem. *284*, 19280–19289. https://doi.org/10.1074/jbc.M109.013102.
87. Menendez, D., Nguyen, T.A., Freudenberg, J.M., Mathew, V.J., Anderson, C.W., Jothi, R., and Resnick, M.A. (2013). Diverse stresses dramatically alter genome-wide p53 binding and transactivation landscape in human cancer cells. Nucleic Acids Res. *41*, 7286–7301. https://doi.org/10.1093/nar/gkt504.
88. Su, D., Wang, X., Campbell, M.R., Song, L., Safi, A., Crawford, G.E., and Bell, D.A. (2015). Interactions of chromatin context, binding site sequence content, and sequence evolution in stress-induced p53 occupancy and transactivation. PLoS Genet. *11*, e1004885. https://doi.org/10.1371/journal.pgen.1004885.
89. Polager, S., and Ginsberg, D. (2009). p53 and E2f: partners in life and death. Nat. Rev. Cancer *9*, 738–748. https://doi.org/10.1038/nrc2718.
90. Deffie, A., Wu, H., Reinke, V., and Lozano, G. (1993). The tumor suppressor p53 regulates its own transcription. Mol. Cell Biol. *13*, 3415–3423. https://doi.org/10.1128/mcb.13.6.3415-3423.1993.
91. Mosner, J., Mummenbrauer, T., Bauer, C., Sczakiel, G., Grosse, F., and Deppert, W. (1995). Negative feedback regulation of wild-type p53 biosynthesis. EMBO J. *14*, 4442–4449. https://doi.org/10.1002/j.1460-2075.1995.tb00123.x.
92. Wang, S., and El-Deiry, W.S. (2006). p73 or p53 directly regulates human p53 transcription to maintain cell cycle checkpoints. Cancer Res. *66*, 6982–6989. https://doi.org/10.1158/0008-5472.CAN-06-0511.
93. Boone, J.Q., and Doe, C.Q. (2008). Identification of Drosophila type II neuroblast lineages containing transit amplifying ganglion mother cells. Dev. Neurobiol. *68*, 1185–1195. https://doi.org/10.1002/dneu.20648.
94. Bello, B.C., Izergina, N., Caussinus, E., and Reichert, H. (2008). Amplification of neural stem cell proliferation by intermediate progenitor cells in Drosophila brain development. Neural Dev. *3*, 5. https://doi.org/10.1186/1749-8104-3-5.
95. Rives-Quinto, N., Franco, M., de Torres-Jurado, A., and Carmena, A. (2017). Synergism between canoe and scribble mutations causes tumor-like overgrowth via Ras activation in neural stem cells and epithelia. Development *144*, 2570–2583. https://doi.org/10.1242/dev.148171.
96. Carmena, A. (2018). Compromising asymmetric stem cell division in Drosophila central brain: Revisiting the connections with tumorigenesis. Fly *12*, 71–80. https://doi.org/10.1080/19336934.2017.1416277.
97. Manzanero-Ortiz, S., de Torres-Jurado, A., Hernández-Rojas, R., and Carmena, A. (2021). Pilot RNAi Screen in *Drosophila* Neural Stem Cell Lineages to Identify Novel Tumor Suppressor Genes Involved in Asymmetric Cell Division. Int. J. Mol. Sci. *22*, 11332. https://doi.org/10.3390/ijms222111332.
98. Sousa-Nunes, R., and Somers, W.G. (2010). Phosphorylation and dephosphorylation events allow for rapid segregation of fate determinants during Drosophila neuroblast asymmetric divisions. Commun. Integr. Biol. *3*, 46–49.
99. Benetka, W., Mehlmer, N., Maurer-Stroh, S., Sammer, M., Koranda, M., Neumüller, R., Betschinger, J., Knoblich, J.A., Teige, M., and Eisenhaber, F. (2008). Experimental testing of predicted myristoylation targets involved in asymmetric cell division and calcium-dependent signalling. Cell Cycle *7*, 3709–3719.
100. Krahn, M.P., Klopfenstein, D.R., Fischer, N., and Wodarz, A. (2010). Membrane targeting of Bazooka/PAR-3 is mediated by direct binding to phosphoinositide lipids. Curr. Biol. *20*, 636–642. https://doi.org/10.1016/j.cub.2010.01.065.
101. Cai, Y., Chia, W., and Yang, X. (2001). A family of snail-related zinc finger proteins regulates two distinct and parallel mechanisms that mediate Drosophila neuroblast asymmetric divisions. EMBO J. *20*, 1704–1714. https://doi.org/10.1093/emboj/20.7.1704.
102. Rust, K., Tiwari, M.D., Mishra, V.K., Grawe, F., and Wodarz, A. (2018). Myc and the Tip60 chromatin remodeling complex control neuroblast maintenance and polarity in Drosophila. EMBO J. *37*, e98659. https://doi.org/10.15252/embj.201798659.
103. Chang, K.C., Garcia-Alvarez, G., Somers, G., Sousa-Nunes, R., Rossi, F., Lee, Y.Y., Soon, S.B., Gonzalez, C., Chia, W., and Wang, H. (2010). Interplay between the transcription factor Zif and aPKC regulates neuroblast polarity and self-renewal. Dev. Cell *19*, 778–785. https://doi.org/10.1016/j.devcel.2010.10.007.
104. Rust, K., and Wodarz, A. (2021). Transcriptional Control of Apical-Basal Polarity Regulators. Int. J. Mol. Sci. *22*, 12340. https://doi.org/10.3390/ijms222212340.
105. Guo, M., Jan, L.Y., and Jan, Y.N. (1996). Control of daughter cell fates during asymmetric division: interaction of Numb and Notch. Neuron *17*, 27–41. https://doi.org/10.1016/s0896-6273(00)80278-0.
106. Spana, E.P., and Doe, C.Q. (1996). Numb antagonizes Notch signaling to specify sibling neuron cell fates. Neuron *17*, 21–26. https://doi.org/10.1016/s0896-6273(00)80277-9.
107. McGill, M.A., and McGlade, C.J. (2003). Mammalian numb proteins promote Notch1 receptor ubiquitination and degradation of the Notch1 intracellular domain. J. Biol. Chem. *278*, 23196–23203. https://doi.org/10.1074/jbc.M302827200.
108. Pece, S., Serresi, M., Santolini, E., Capra, M., Hulleman, E., Galimberti, V., Zurrida, S., Maisonneuve, P., Viale, G., and Di Fiore, P.P. (2004). Loss of negative regulation by Numb over Notch is relevant to human breast carcinogenesis. J. Cell Biol. *167*, 215–221. https://doi.org/10.1083/jcb.200406140.
109. Colaluca, I.N., Tosoni, D., Nuciforo, P., Senic-Matuglia, F., Galimberti, V., Viale, G., Pece, S., and Di Fiore, P.P. (2008). NUMB controls p53 tumour suppressor activity. Nature *451*, 76–80. https://doi.org/10.1038/nature06412.
110. Tosoni, D., Zecchini, S., Coazzoli, M., Colaluca, I., Mazzarol, G., Rubio, A., Caccia, M., Villa, E., Zilian, O., Di Fiore, P.P., and Pece, S. (2015). The Numb/p53 circuitry couples replicative self-renewal and tumor suppression in mammary epithelial cells. J. Cell Biol. *211*, 845–862. https://doi.org/10.1083/jcb.201505037.
111. Faraldo, M.M., and Glukhova, M.A. (2015). Regulating the regulator: Numb acts upstream of p53 to control mammary stem and progenitor cell. J. Cell Biol. *211*, 737–739. https://doi.org/10.1083/jcb.201510104.
112. Liu, J., Zhang, C., Wang, X.L., Ly, P., Belyi, V., Xu-Monette, Z.Y., Young, K.H., Hu, W., and Feng, Z. (2014). E3 ubiquitin ligase TRIM32 negatively regulates tumor suppressor p53 to promote tumorigenesis. Cell Death Differ. *21*, 1792–1804. https://doi.org/10.1038/cdd.2014.121.
113. Izumi, H., and Kaneko, Y. (2014). Trim32 facilitates degradation of MYCN on spindle poles and induces asymmetric cell division in human neuroblastoma cells. Cancer Res. *74*, 5620–5630. https://doi.org/10.1158/0008-5472.CAN-14-0169.
114. Wang, M., Luo, W., Zhang, Y., Yang, R., Li, X., Guo, Y., Zhang, C., Yang, R., and Gao, W.Q. (2020). Trim32 suppresses cerebellar development and tumorigenesis by degrading Gli1/sonic hedgehog signaling. Cell Death Differ. *27*, 1286–1299. https://doi.org/10.1038/s41418-019-0415-5.
115. Bawa, S., Piccirillo, R., and Geisbrecht, E.R. (2021). TRIM32: A Multifunctional Protein Involved in Muscle Homeostasis, Glucose Metabolism, and Tumorigenesis. Biomolecules *11*, 408. https://doi.org/10.3390/biom11030408.
116. Schwamborn, J.C., Berezikov, E., and Knoblich, J.A. (2009). The TRIM-NHL protein TRIM32 activates microRNAs and prevents self-renewal in mouse neural progenitors. Cell *136*, 913–925. https://doi.org/10.1016/j.cell.2008.12.024.
117. Krajewska, M., Krajewski, S., Zapata, J.M., Van Arsdale, T., Gascoyne, R.D., Berern, K.,

McFadden, D., Shabaik, A., Hugh, J., Reynolds, A., et al. (1998). TRAF-4 expression in epithelial progenitor cells. Analysis in normal adult, fetal, and tumor tissues. Am. J. Pathol. *152*, 1549–1561.

118. Camilleri-Broët, S., Cremer, I., Marmey, B., Comperat, E., Viguié, F., Audouin, J., Rio, M.C., Fridman, W.H., Sautès-Fridman, C., and Régnier, C.H. (2007). TRAF4 overexpression is a common characteristic of human carcinomas. Oncogene *26*, 142–147. https://doi.org/10.1038/sj.onc.1209762.
119. Wu, L., Chen, X., Zhao, J., Martin, B., Zepp, J.A., Ko, J.S., Gu, C., Cai, G., Ouyang, W., Sen, G., et al. (2015). A novel IL-17 signaling pathway controlling keratinocyte proliferation and tumorigenesis via the TRAF4-ERK5 axis. J. Exp. Med. *212*, 1571–1587. https://doi.org/10.1084/jem.20150204.
120. Wang, H., Somers, G.W., Bashirullah, A., Heberlein, U., Yu, F., and Chia, W. (2006). Aurora-A acts as a tumor suppressor and regulates self-renewal of Drosophila neuroblasts. Genes Dev. *20*, 3453–3463. https://doi.org/10.1101/gad.1487506.
121. Drosten, M., Sum, E.Y.M., Lechuga, C.G., Simón-Carrasco, L., Jacob, H.K.C., García-Medina, R., Huang, S., Beijersbergen, R.L., Bernards, R., and Barbacid, M. (2014). Loss of p53 induces cell proliferation via Ras-independent activation of the Raf/Mek/Erk signaling pathway. Proc. Natl. Acad. Sci. USA *111*, 15155–15160. https://doi.org/10.1073/pnas.1417549111.
122. Drosten, M., and Barbacid, M. (2016). Ras and p53: An unsuspected liaison. Mol. Cell. Oncol. *3*, e996001. https://doi.org/10.1080/23723556.2014.996001.
123. Meletis, K., Wirta, V., Hede, S.M., Nistér, M., Lundeberg, J., and Frisén, J. (2006). p53 suppresses the self-renewal of adult neural stem cells. Development *133*, 363–369. https://doi.org/10.1242/dev.02208.
124. Hall, P.A., and McCluggage, W.G. (2006). Assessing p53 in clinical contexts: unlearned lessons and new perspectives. J. Pathol. *208*, 1–6. https://doi.org/10.1002/path.1913.
125. Martín-Bermudo, M.D., Martinez, C., Rodriguez, A., and Jimenez, F. (1991). Distribution and function of the lethal of scute gene product during early neurogenesis in Drosophila. Development *113*, 445–454.
126. Carmena, A., Bate, M., and Jiménez, F. (1995). Lethal of scute, a proneural gene, participates in the specification of muscle progenitors during Drosophila embryogenesis. Genes Dev. *9*, 2373–2383.
127. Frasch, M., Hoey, T., Rushlow, C., Doyle, H., and Levine, M. (1987). Characterization and localization of the even-skipped protein of Drosophila. EMBO J. *6*, 749–759.
128. Kurtz, P., Jones, A.E., Tiwari, B., Link, N., Wylie, A., Tracy, C., Krämer, H., and Abrams, J.M. (2019). Drosophila p53 directs nonapoptotic programs in postmitotic tissue. Mol. Biol. Cell *30*, 1339–1351. https://doi.org/10.1091/mbc.E18-12-0791.
129. Koenecke, N., Johnston, J., Gaertner, B., Natarajan, M., and Zeitlinger, J. (2016). Genome-wide identification of Drosophila dorso-ventral enhancers by differential histone acetylation analysis. Genome Biol. *17*, 196. https://doi.org/10.1186/s13059-016-1057-2.
130. Koenecke, N., Johnston, J., He, Q., Meier, S., and Zeitlinger, J. (2017). Drosophila poised enhancers are generated during tissue patterning with the help of repression. Genome Res. *27*, 64–74. https://doi.org/10.1101/gr.209486.116.
131. Rajan, A., Anhezini, L., Rives-Quinto, N., Chhabra, J.Y., Neville, M.C., Larson, E.D., Goodwin, S.F., Harrison, M.M., and Lee, C.Y. (2023). Low-level repressive histone marks fine-tune gene transcription in neural stem cells. Elife *12*, e86127. https://doi.org/10.7554/eLife.86127.
132. Robinson, J.T., Thorvaldsdóttir, H., Winckler, W., Guttman, M., Lander, E.S., Getz, G., and Mesirov, J.P. (2011). Integrative genomics viewer. Nat. Biotechnol. *29*, 24–26. https://doi.org/10.1038/nbt.1754.

STAR★METHODS

KEY RESOURCES TABLE

REAGENT or RESOURCE	SOURCE	IDENTIFIER
Antibodies		
Rabbit anti-Ase	Carmena lab[95]	NA
Guinea pig anti-Dpn	Carmena lab[95]	NA
Mouse anti-γTub	Sigma-Aldrich	Sigma-Aldrich Cat# T5326; RRID: AB_532292
Rabbit anti-PH3	Millipore	Millipore Cat# 06-570; RRID: AB_310177
Mouse anti-PH3	Millipore	Millipore Cat# 05-806; RRID: AB_310016
Mouse anti-Dlg1	Developmental Studies Hybridoma Bank	DSHB Cat# DLG1; RRID: AB_2314321
Mouse anti-β-galactosidase	Promega	Promega Cat# 73781; RRID: AB_430877
Rabbit anti-Eve	A gift from M. Frasch	NA
Rabbit anti-PKCζ	Santa Cruz Biotechnology	Santa Cruz Biotechnology Cat# sc-216; RRID: AB_2300359
Goat anti-Numb	Santa Cruz Biotechnology	Santa Cruz Biotechnology Cat# sc-23579; RRID: AB_653503
Guinea pig anti-Par-6	A gift from A. Wodarz	NA
Rabbit anti-Brat	A gift from J. Knoblich	NA
Mouse IgG Isotype Control	Thermo Fisher Scientific	Cat# 31903; RRID: AB_10959891
Mouse anti-p53	Developmental Studies Hybridoma Bank	DSHB Cat# p53 7A4; RRID: AB_579786
Secondary antibodies conjugated to fluorescent dyes Goat anti-Rabbit Alexa Fluor 546	Invitrogen	Cat# A-11035; RRID: AB_2534093
Secondary antibodies conjugated to fluorescent dyes Goat anti-Rabbit Alexa Fluor 647	Invitrogen	Cat# A32733; RRID: AB_2633282
Secondary antibodies conjugated to fluorescent dyes Goat anti-Mouse Alexa Fluor 488	Invitrogen	Cat# A32723; RRID: AB_2633275
Secondary antibodies conjugated to fluorescent dyes Goat anti-Mouse Alexa Fluor 647	Invitrogen	Cat# A32728; RRID: AB_2633277
Secondary antibodies conjugated to fluorescent dyes Goat anti-Guinea Pig Alexa Fluor 555	Invitrogen	Cat# A-21435; RRID: AB_2535856
Secondary antibodies conjugated to fluorescent dyes Goat anti-Guinea Pig Alexa Fluor 647	Invitrogen	Cat# A-21450; RRID: AB_2735091
Secondary antibodies conjugated to fluorescent dyes Cy3 anti-Goat	Jackson ImmunoResearch	Cat# 805-165-180; RRID: AB_2340880
Secondary antibodies conjugated to Biotin Biotin anti-Rabbit	Jackson ImmunoResearch	Cat# 711-065-152; RRID: AB_2340593
Secondary antibodies conjugated to Biotin Biotin anti-Mouse	Jackson ImmunoResearch	Cat# 115-065-166; RRID: AB_2338569

(*Continued on next page*)

Continued

REAGENT or RESOURCE	SOURCE	IDENTIFIER
Chemicals, peptides, and recombinant proteins		
Formaldehyde (FA)	EMD Millipore Corporation	Cat # 1.04003.1000
Paraformaldehyde (PFA)	Electron Microscopy Sciences (EMSO	Cat# 15710
Triton CF10	Fluka	Cat# 93416
Vectastain ABC kit	Vector labs	Cat# PK-6100
Vectashield Antifade Mounting Medium for Fluorescence	Vector labs	Cat# H-1000
TRI Reagent	Invitrogen	Cat# AM9738
DNAse	Thermo Scientific	Cat# EN0521
NZY Reverse Transcriptase	NZYTech	Cat# MB12401
SuperScriptTM III Reverse Transcriptase	Invitrogen	Cat# 1808044
Oligo(dT) primer mix	NZYTech	Cat# MB12801
Oligo(dT) primer mix	Invitrogen	Cat# 184181-020
NZY Supreme qPCR Green Master Mix, ROX Plus	NZYTech	Cat# MB440022
Power SYBR Green PCR Master Mix	Applied Biosystems	Cat# PN4367218
Protease inhibitor cocktail	Sigma	Cat# 539137
ProtG/Sepharose	Sigma	Cat# P3296
Power SYBR Green	Applied Biosystems	Cat# 4367659
Experimental models: Organisms/strains		
D. melanogaster: $p53^{E8}$	Chung lab[74]	NA
D. melanogaster: hs-FLP	Bloomington Drosophila Stock Center	BDSC: 6
D. melanogaster: Dll-Gal4 UAS-CD8::GFP	Bloomington Drosophila Stock Center	BDSC: 64307
D. melanogaster: FRT82B $p53^{E8}$	Recombinant from this work	NA
D. melanogaster: UAS-Ras^{V12} FRT82B $scrib^{2}$	A gift from G. Halder/H. Richardson	NA
D. melanogaster: UAS-$p53^{RNAi}$	Bloomington Drosophila Stock Center	BDSC: 41638
D. melanogaster: wor-Gal4	Bloomington Drosophila Stock Center	BDSC: 56553
D. melanogaster: UAS-CD8::GFP	Bloomington Drosophila Stock Center	BDSC: 5137
Oligonucleotides		
GCA GCA TTA ATC AGA ACA TC *numb* (Fw primer)	This paper	NA
ATG GAG CGT CTG ATA TGT GG *numb* (Rev primer)	This paper	NA
GCA AGG TGA TGC GTG TGA TC *brat* (Fw primer)	This paper	NA
TGT CGC TGA TGA AGA TCT CC *brat* (Rev primer)	This paper	NA
GCA CTC TGT TGT GGA AGA TC *Traf4* (Fw primer)	This paper	NA
AGT GTG AAG GTG ATG GAG TGC *Traf4* (Rev primer)	This paper	NA
TCG ATC ATG AAG TGC GAC GT *Act88F* (Fw primer)	This paper	NA
CGG AGT ACT TCC TCT CGG GT *Act88F* (Rev primer)	This paper	NA
TAA ATT CGA CTC GAC TCA CGG T *GADPH* (Fw primer)	This paper	NA
CTC CAC CAC ATA CTC GGC TC *GADPH* (Rev primer)	This paper	NA
GTGGCAGCCGGTCGAA *3'UTR* (Fw primer, ChIP)	This paper	NA
CAGCCAAAGCGGATGCA *3'UTR* (Rev primer, ChIP)	This paper	NA
CGCTTGTACTTGCATCATTCG *p53PROM* (Fw primer, ChIP)	This paper	NA
GCGCCTTGGCTGGATAAAC *p53PROM* (Rev primer, ChIP)	This paper	NA
GAATGGTTCCGTGGTTCGTTG *brat* (Fw primer, ChIP)	This paper	NA
AACAATTACGCCAAGCGTTGA *brat* (Rev primer, ChIP)	This paper	NA
GTGCAAAGGAGAGGGGTTAC *Traf4* (Fw primer, ChIP)	This paper	NA

(*Continued on next page*)

Continued

REAGENT or RESOURCE	SOURCE	IDENTIFIER
ACGCCAATTCCTTGGAGCCAG *Traf4* (Rev primer, ChIP)	This paper	NA
ACCGAGACAAGCTCGATTGG *numb* (Fw primer, ChIP)	This paper	NA
ATTACCCCTCTTTTGGCGGG *numb* (Rev primer, ChIP)	This paper	NA
Software and algorithms		
GEO Browser - GEO NCBI	https://www.ncbi.nlm.nih.gov/geo/browse/	
ENCODE Consortium Project	https://www.encodeproject.org/	
Integrative Genome browser IGV	https://igv.org/	
SigmaPlot 12.0 Software	https://sigmaplot.software.informer.com/12.0/	
Fiji/ImageJ	Open Resourse	
Adobe Photoshop CS6	Adobe Inc.	

EXPERIMENTAL MODEL AND STUDY PARTICIPANT DETAILS

Our model system in this study has been *Drosophila melanogaster*.

Drosophila strains and genetics

The fly stocks used in this work were from the Bloomington *Drosophila* Stock Center (BDSC) unless otherwise noted: *white (w)*, was used as a wild-type control fly strain; $p53^{E8}$ [74]; *hs-FLP* (BDSC: #6); *Dll-Gal4 UAS-CD8::GFP* (BDSC: #64307); *FRT82B tub-Gal80; FRT82B* $p53^{E8}$ (this work); *UAS-Ras*^{V12} *FRT82B scrib*^{2} (from G. Halder/H. Richardson); *FRT82B*; *UAS-p53*^{RNAi} (BDSC: #41638); *wor-Gal4* (BDSC:56553); *UAS-CD8::GFP* (BDSC: 5137).

Balancer chromosomes containing *lacZ* transgenes or a Tubby (Tb) dominant marker were used to identify homozygous mutant embryos or larvae, respectively.

Drosophila husbandry

All the fly stocks were raised and kept in 18°C or 25°C incubators. Experimental temperatures for the assays were maintained using 25°C or 29°C incubators. The *Gal-4 x UAS* crosses (i.e. *wor-Gal4; UAS-CD8::GFP* x *UAS-p53*^{RNAi}) in Figures S2B and S2C were carried out at 25°C for 2 days and then transferred to a new tube and left at 29°C until larvae of the proper stage (third instar, L3, larvae) developed. All stocks were kept in bottles containing standard molasses fly food. We are not aware about the influence (or association) of sex, gender or both on the results of this study.

METHOD DETAILS

Immunohistochemistry, immunofluorescence and microscopy

Embryos or larval brains were fixed and stained by modification of standard protocols.[125,126] In brief, dechorionated embryos or dissected late L3 brains were fixed in 4% formaldehyde in phosphate-buffered saline (PBS, pH 7,4) during 20 minutes at room temperature (RT) in an orbital shaker. The following primary Abs were used: rabbit anti-Ase 1:100,[95] guinea pig anti-Dpn 1:2000,[95] mouse anti-γ-Tubulin 1:400 (*Sigma-Aldrich*, T5326), rabbit anti-phospho-Histone H3 1:400 (*Millipore*, 06-570), mouse anti-phospho-Histone H3 1:2000 (*Millipore*, 05-806), mouse anti-Dlg1 1:25 (*DSHB*), mouse anti-β-galactosidase from 1:200 to 1:8000 (for immunofluorescence and DAB staining, respectively) (*Promega*, Z3781), rabbit anti-Eve 1:3000,[127] rabbit anti-PKCζ 1:100 (*Santa Cruz Biotechnology*, sc-216), goat anti-Numb 1:200 (*Santa Cruz Biotechnology*, sc-23579), guinea pig anti Par-6 1:1000 (a gift from A. Wodarz) and rabbit anti-Brat 1:200 (a gift from J. Knoblich).

The following secondary Abs conjugated with fluorescent dyes: Alexa Fluor 488, Alexa Fluor 546, Alexa Fluor 633 and Alexa Fluor 647 (all from *Invitrogen*) and Cy3 (*Jackson ImmunoResearch*) 1:400 were used. VECTASHIELD Antifade Mounting Medium for Fluorescence (*Vector labs*) was used for embryos or brain larvae immunofluorescences. 1:200 goat-biotinylated anti-mouse and 1:200 donkey-biotinylated anti-rabbit (*Vector labs*) were used for embryo immunohistochemistry followed by an incubation with the Vectastain ABC kit (*Vector labs*). After oxidation of DAB by using 0.01% of peroxidase, embryos were rinsed several times in PBT followed by a dehydration process and finally mounted with a drop of Epon.

Immunohistochemistry was visualized using Nomarski Optics on a Carl Zeiss microscope (Axio Imager.A1). Images of ventral view embryos were taken with a 63x/1.25 oil objective. Images were assembled using Adobe Photoshop CS6 program. Fluorescence images from Figures 2A and 2B were recorded by using an Inverted Leica laser-scanning spectral confocal microscope TCS SP2 (Leica Spectral Confocal acquisition software). The rest of fluorescence images were recorded using a Super-resolution Inverted Confocal Microscope Zeiss LSM 880-Airyscan Elyra PS.1. Images were analyzed using the image processing package FIJI from ImageJ and assembled using Adobe Photoshop CS6 program.

MARCM clones

Clones in the brain were generated crossing *hsFLP; Dll-Gal4 UAS-CD8::GFP; FRT82B tubGal80* females with males of the different genotypes specified, including *UAS-p53^{RNAi}; FRT82B//UAS-Ras^{V12} FRT82B scrib^{2}// UAS-p53^{RNAi}; UAS-Ras^{V12} FRT82B scrib^{2}* and *FRT82B* as control males. The clones were identified by the presence of CD8::GFP. hsFLP was induced for 2 h at 37°C in late first/early second instar larvae and clones were analyzed in late third instar larvae.

qRTPCR

To quantify RNA levels, total RNA was extracted from 16 halved *Drosophila* larvae using TRI Reagent (*Invitrogen, AM9738*). Briefly, samples were incubated 5 min at RT, 100 µl BCP (1-bromo-3-chloropropane) / mL TRI Reagent was added and incubated again for 15 min at RT. After centrifugation, the aqueous phase was collected and 0.7 volumes of isopropanol / mL TRI Reagent were added. After a centrifugation, pellet was washed with 70% Ethanol, resuspended in TE and quantified using a Nanodrop (*Thermo Scientific, ND-1000*). RNA was treated with DNAse (*Thermo Scientific, EN0521*) and reverse transcripted with NZY Reverse Transcriptase (*NZYTech, MB12401*). For Numb PCRs, SuperScriptTM III Reverse Transcriptase (*Invitrogen, 1808044*) was used. Oligo(dT) primer mix (*NZYTech, MB12801* or *Invitrogen, 184181-020* in the case of Numb) were used. Quantitative real time PCR (qRT-PCR) was performed using NZY Supreme qPCR Green Master Mix, ROX Plus (*NZYTech, MB440022*) or Power SYBR Green PCR Master Mix (*Applied Biosystems, PN4367218*) in the case of Numb amplification, following established protocols with 60°C for annealing/extension and 40 Cycles of amplification, on a QuantStudio™ 3 apparatus (*Applied Biosystems*). Act88F and GADPH primers were used for mRNA normalization. Comparative qPCRs were performed in at least three replicates and the relative expression was calculated using the comparative ΔΔCt method. qRT-PCR primers are listed in the Table.

ChIP experiments

Drosophila control (*w*) larvae were raised at 25°C until late third instar stage for brain dissection. Around 200 brains (with carcasses) were dissected in cold PBS and fixed with 1 ml cross-linking solution (1.8 % formaldehyde, 50 mM Hepes pH 8.1 mM EDTA, 0.5 mM EGTA, 100 mM NaCl). The cross-linking solution was changed 3-4 times during fixation. The cross-linking was discontinued by washing for 3 min in 1ml PBS/0.01 % Triton X-100/125 mM glycine with 3-4 changes. Fixed carcasses were washed for 10 min in 1 ml Wash A solution (10 mM Hepes pH 7.6, 10 mM EDTA, 0.5 mM EGTA, 0.25 % Triton X-100) and, subsequently, for 10 min in 1 ml Wash B solution (10 mM Hepes pH7.6, 200 mM NaCl, 1m M EDTA, 0.5 mM EGTA, 0.01 % Triton X-100) changing the wash solution 3-4 times. Fine dissection of the brains was carried out in cold Wash B and samples were homogenized in 300 µl RIPA buffer (140 mM NaCl, 10 mM Tris-HCl pH 8.0, 1 mM EDTA, 1 %Triton X-100, 0.1 % SDS, 0.1 % sodium deoxycholate, 1 mM PMSF, 1 x Complete protease inhibitor cocktail (*Sigma*, 539137) with 0.5 % N-Laurylsarcosine) during 15 min on ice, pipetting up and down several times. DNA was fragmented using a Biorruptor with 12 cycles of sonication for 30 s and interval for 30 s. This sonication yields genomic DNA fragments of around 500 bp. Sonicated lysate was centrifuged at 4°C for 25 min at 14000 rpm to remove debris and diluted with RIPA buffer (without N-Laurylsarcosine) containing proteinase inhibitors to 2 brains per 10µl. Samples were precleared with 100µl of pretreated ProtG/Sepharose (*Sigma, P3296*) for 1 hr at 4°C. After centrifugation to eliminate the beads, 1ml precleared lysate were used for each IP and 100µl (10%) of it was saved for Input. The rest was separated into two aliquots of 450 µl each and incubated overnight at 4°C with 3 µg of a Mouse IgG Isotype Control (*Thermo Fisher Scientific, 31903*) or a Mouse anti-p53 (DSHB, p53 7A4) Abs, respectively. Overnight preblocked protG/Sepharose beads with 2 mg/ml BSA, 0.5 mg/ml Salmon Test DNA in RIPA buffer +PI were added for an extra 4 h of incubation at 4°C. Beads were then washed once with RIPA buffer and 4 times with high salt wash buffer (0.1% SDS, 1% Triton X-100, 2mM EDTA, 20mM Tris–HCl pH8, 500 mM NaCl), once with LiCl wash buffer (1% NP40, 1% sodium deoxycholate, 1mM EDTA, 10mM Tris–HCl pH8, 0.25M LiCl), twice with TE buffer (10mM Tris-HCl pH8, 1mM EDTA), and then eluted and re-eluted with 200 µl each of freshly made elution buffer (1% SDS, 0.1M NaHCO3). Input was diluted by adding 300 µl of Elution buffer. 5M NaCl to a final concentration of 0.3M was added into all tubes before incubation at 65°C overnight to reverse the crosslinking. 2µl 10mg/ml RNase was added and incubated 1 h at 37°C; then, 10µl 0.5M EDTA, 20µl 1 M Tris pH 6.5 and 1µl Proteinase K 20mg/ml were added and incubated 1 h at 45°C. Samples were cleaned up with phenol:chloroform, precipitated with EtOH and resuspended in 50 µl of water. Purified DNA was used for region-specific quantification by qPCR using Power SYBR Green (*Applied Biosystems*, 4367659) in triplicates per ChIP. ChIP primers are listed in the following Table.

ChIPseq data processing and visualization

The following *Drosophila* genome-wide binding data sets were used: p53 embryos (4.5-5.5 hours) and p53 heads (1—2 weeks) from GEO GSE109292,[128] H3K27ac (embryo) from GEO GSM1689671,[129,130] and H3K4m3 (larva) from GEO GSE218253.[131] ChIP-seq for the Transcription Factor E2F2 (embryo 0-24hours) and p53-MiMic GFP (embryo 0-24hours) were obtained from the ENCODE Consortium Project with accession numbers ENCFF070DKY and ENCFF187EJC respectively. The Integrative Genome browser IGV[132] was used to visualize the data set of p53 RE sequences in the *Drosophila melanogaster* genome version Dm6.

QUANTIFICATION AND STATISTICAL ANALYSIS

Statistical analyses were carried out with SigmaPlot 12.0 Software. To assume statistical significance, p-values were determined below 0.05. The data were first analyzed using the Shapiro-Wilk test to determine whether the sample followed a normal distribution. Parametric t-test or a

nonparametric two-tailed Mann Whitney U test and Kruskal-Wallis test for those that did not follow a normal distribution were used to compare statistical differences between two different groups. To determine the equality of proportion between different groups, a Chi-squared test (with Yates correction) was applied.

For most experiments, images data graphic representation was done using simple bars; box plots with whiskers were used in Figures 4 and S3B. The specific test used, experimental sample size (n) and the *p*-value are indicated in the figure or figure legend; * $p < 0.05$, ** $p < 0.01$, *** $p < 0.001$, ns: not significant ($p > 0.05$).